New Zealand Journal of Geology & Geophysics, 2004, Vol. 47: 787–807
0028–8306/04/4704–0787

Textural variations in Neogene pelagic carbonate ooze at DSDP Site 593, southern Tasman Sea, and their paleoceanographic implications

PENELOPE J. COOKE[1]
CAMPBELL S. NELSON[1]
MARTIN P. CRUNDWELL[1,2]
BRAD D. FIELD[2]
E. SHIRLEY ELKINGTON[1]
HAROLD H. STONE[1]

[1]Department of Earth Sciences
University of Waikato
Private Bag 3105
Hamilton, New Zealand
email: p.cooke@waikato.ac.nz

[2]Institute of Geological & Nuclear Sciences
P.O. Box 30 368
Lower Hutt, New Zealand

Abstract Changes in Neogene sediment texture in pelagic carbonate-rich oozes on the Challenger Plateau, southern Tasman Sea, are used to infer changes in depositional paleocurrent velocities. The most obvious record of textural change is in the mud:sand ratio. Increases in the sand content are inferred to indicate a general up-core trend towards increasing winnowing of sediments resulting from increasing flow velocity of Southern Component Intermediate Water (SCIW), the forerunner of Antarctic Intermediate Water. In particular, the intervals c. 19–14.5 Ma, c. 9.5–8 Ma, and after 5 Ma are suggested to be times of increased SCIW velocity and strong sediment winnowing. Within the mud fraction, the fine silt to coarse clay sizes from 15.6 to 2 μm make the greatest contribution to the sediments and are composed of nannofossil plates. During extreme winnowing events it is the fine silt to very coarse clay material (13–3 μm) within this range that is preferentially removed, suggesting the 10 μm cohesive silt boundary reported for siliciclastic sediments does not apply to calcitic skeletal grains. The winnowed sediment comprises coccolithophore placoliths and spheres, represented by a mode at 4–7 μm.

Further support for seafloor winnowing is gained from the presence in Hole 593 of a condensed sedimentary section from c. 18 to 14 Ma where the sand content increases to c. 20% of the bulk sample. Associated with the condensed section is a 6 m thick orange unit representing sediments subjected to particularly oxygen-rich, late early to early middle Miocene SCIW. Together these are inferred to indicate increased SCIW velocity resulting in winnowed sediment associated with faster arrival of oxygen-rich surface water subducted to form SCIW. Glacial development of Antarctica has been recorded from many deep-sea sites, with extreme glacials providing the mechanism to increase watermass flow. Miocene glacial zones Mi1b–Mi6 are identified in an associated oxygen isotope record from Hole 593, and correspond with times of particularly invigorated paleocirculation, bottom winnowing, and sediment textural changes.

Keywords Tasman Sea; carbonate; texture; Neogene; DSDP Site 593; winnowing

INTRODUCTION

Climate change and its effects on ocean circulation can only be monitored in ancient sediments using proxy parameters. Sediment texture can be used as a proxy as it provides a means of determining the mechanism of deposition, reworking, and dispersal of sediments in the deep ocean (Gorsline 1984), which in turn can be linked to paleocirculation and paleoclimatic changes. Texturally, silt-sized siliciclastic particles (4–63 μm) have been regarded as particularly diagnostic for studies of deposition and reworking by bottom currents (McCave 1984), and for inferring changes in current velocity over time (e.g., Ellwood et al. 1979). In most textural studies, the non-carbonate sediment fraction has been used because the target watermass was Antarctic Bottom Water (AABW), below the Carbonate Compensation Depth (CCD), and there was a need to eliminate the effects on texture of foraminiferal fragmentation caused by dissolution in carbonate-undersaturated waters.

Studies of the grain-size distribution of carbonate-dominated pelagic sediments have been few in number (e.g., Oser 1972; van Andel 1973; Gardner et al. 1986a; House et al. 1991). This study investigates the nature and possible controls on sediment textural changes in the carbonate-dominated ooze through the earliest Miocene–Holocene interval (c. 19–0 Ma, or most of the Neogene) of core from the mid-latitude, intermediate water depth, Deep Sea Drilling Site (DSDP) 593 in southern Tasman Sea (Fig. 1A). It draws upon both regional and more global paleoceanographic factors to explain the textural variations evident in the high-resolution record.

PHYSICAL SETTING

Geological

Site 593 (40°30.47′S, 167°40.47′E) lies in 1068 m of water near the edge of the Challenger Plateau in the Tasman Sea, 270 km west of New Zealand (Fig. 1A). The bounding Tasman Basin formed about the Tasman Rift system by rifting and seafloor spreading up until c. 55.5 Ma (Sutherland 1994). Post-rift subsidence of Challenger Plateau ceased by the middle Eocene and the plateau depth has remained stable since then (Burns & Andrews 1973; Wood 1993). Northward

G03041; Online publication date 1 December 2004
Received 16 April 2003; accepted 24 February 2004

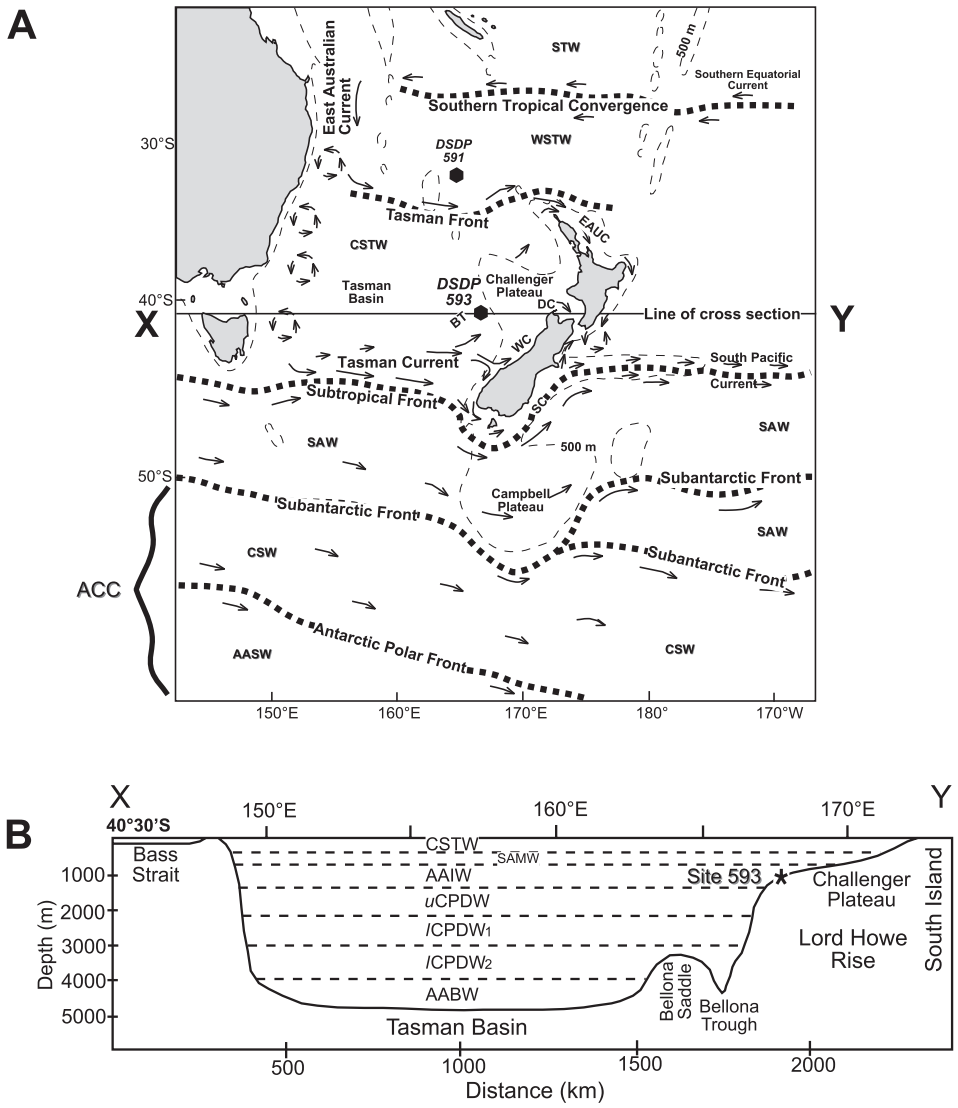

Fig. 1 **A**, Location of DSDP Site 593 (40°30′S, 167°40′E) in the Southwest Pacific showing the main topographic features of the region in relation to the site. The main oceanic fronts and surface watermasses separated by these fronts are included to illustrate the affect that bathymetry has on the frontal positions. Site 591 (31°35′S, 164°27′E in 2131 m water) is located for reference (see text). BT, Bellona Trough; SC, Southland Current; WC, Westland Current; DC, D'Urville Current; EAUC, East Auckland Current; WSTW, Warm Subtropical Water; CSTW, Cool Subtropical Water; SAW, Subantarctic Water; CSW, Circumpolar Surface Water; AASW, Antarctic Surface Water; ACC, Antarctic Circumpolar Current (after Carter et al. 1998a). **B**, Schematic cross-section (X–Y) of the Tasman Basin at 40°30′S, showing the bathymetric position of Site 593 in 1068 m water depth, physiographical features of the basin, and the subsurface watermasses found in the Tasman Sea. SAMW, Subantarctic Mode Water; AAIW, Antarctic Intermediate Water; uCPDW, upper Circumpolar Deep Water; lCPDW, lower Circumpolar Deep Water; AABW, Antarctic Bottom Water (after Wyrtki 1961, 1962; Circum-Pacific Map Project 1978; Rodman & Gordon 1982; Drewry 1983; Heath 1985; Kennett & von der Borch 1986b; Carter et al. 1998b).

migration of the Lord Howe Rise since the Eocene occurred in response to spreading on the Pacific-Antarctic Ridge, shifting Challenger Plateau northward across c. 15° of latitude, to c. 50°S in the early Miocene, and to modern position at 40°S by the Quaternary (Kennett & von der Borch 1986a; Nelson & Cooke 2001).

Oceanographic

Tropical surface waters are transported along the eastern Australian margin by the East Australian Current (EAC), at least half of which deviates as a zonal jet across the Tasman Sea between 30 and 36°S, forming the Tasman Front (Stanton 1973, 1979). The remaining EAC flow continues southward as a series of large eddies, all the while being turned eastwards by the west wind drift along the Subtropical Front at c. 45°S (Fig. 1B) (Bennett 1983; Rochford 1983; Stramma et al. 1995). This eastward surface water flow is the Tasman Current, which deviates off western South Island to flow northward as the eastern margin of the Tasman gyre, and southward as the Southland Current (Heath 1985). As a consequence, cool subtropical surface waters (CSTW) of the southern Tasman Sea flow as a slow anticlockwise gyre, bounded to the north by the Tasman Front and to the south by the Subtropical Front (Heath 1985).

Subsurface watermasses (Fig. 1B) in the southern Tasman Sea enter the region from the south, with the Subantarctic Mode Water (SAMW) flowing between CSTW and Antarctic Intermediate Water (AAIW) (Heath 1985). AAIW enters the

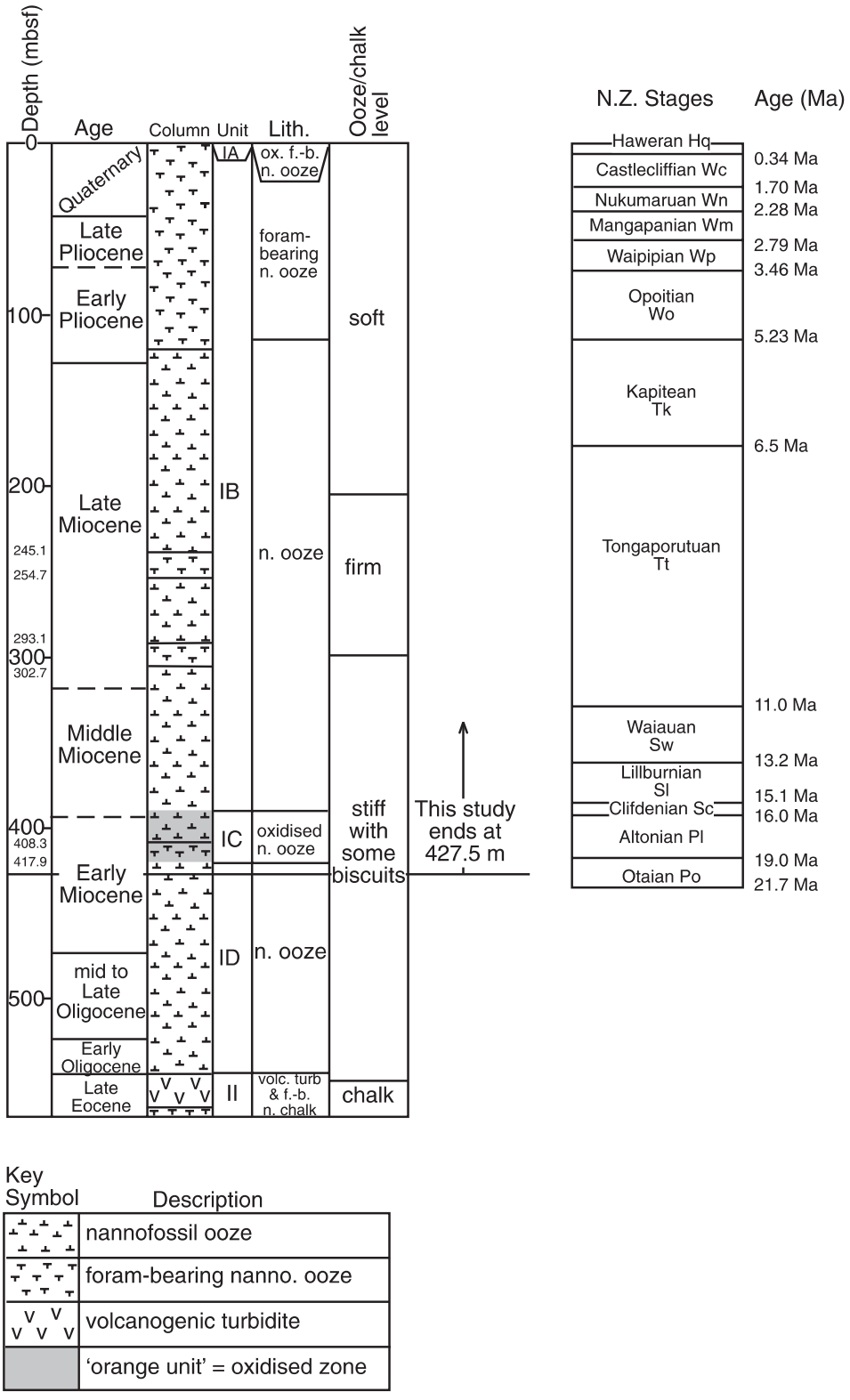

Fig. 2 Site 593 stratigraphy. Unit IA–D = ooze, unit II = volcanogenic turbidite (after Nelson 1986a). Three core sections within the early–late Miocene interval are foram-bearing nannofossil ooze. Some of the ages are slightly different to those reported by Leg 90 Shipboard Scientific Party (1986), a feature of the lack of dating control in the high-carbonate sediments. Absolute ages of New Zealand stages after Morgans et al. (1996).

Tasman Basin from both the south and the north, the latter from between New Zealand and Fiji, and the zone between 30 and 40°S contains AAIW mixed from both sources (Wyrtki 1961). At 1068 m, Site 593 sits within the core of AAIW which spans c. 700–1300 m water depth in the Tasman Sea (Fig. 1B) (Garner 1962, 1967; Garner & Ridgway 1965; Tomczak & Godfrey 1994).

STRATIGRAPHY

Lithology

Sediments at Site 593 comprise largely undifferentiated latest Eocene–Quaternary, white to grey nannofossil ooze or foram-bearing nannofossil ooze (Fig. 2) (Nelson 1986a). A notable feature in this ooze record is the early–middle

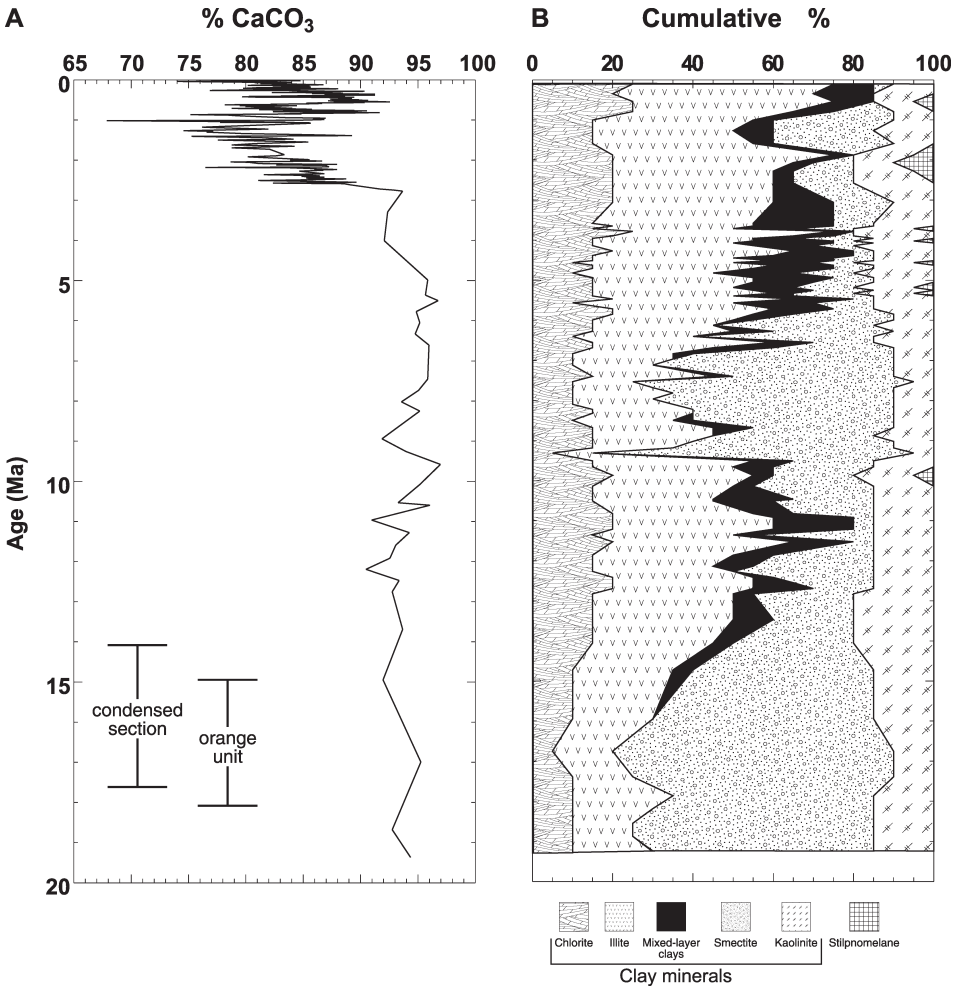

Fig. 3 **A**, Carbonate content of the Neogene section of Hole 593 sediments (after Mycke et al. 1986; unpubl. data). **B**, Composition of the clay fraction through the Neogene section of Hole 593 where the chemically mature clays (smectite and kaolinite) indicate chemical weathering on land, and the chemically immature clays (illite and chlorite) indicate physical weathering. The small amount of stilpnomelane is inferred to originate from the weathering of uplifted, South Island Mesozoic metamorphic terranes containing this micaceous mineral (Robert et al. 1986).

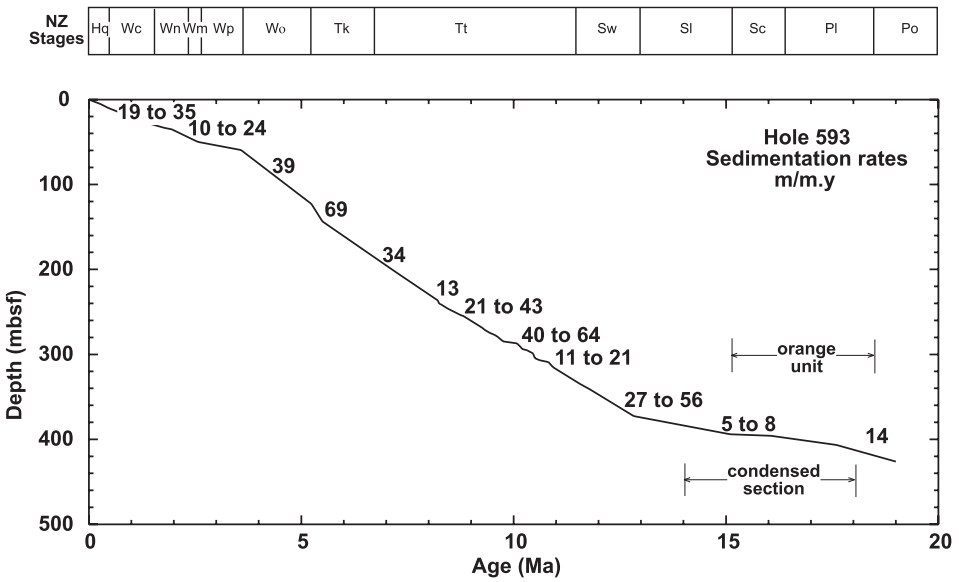

Fig. 4 Hole 593 Neogene sedimentation rates based on the absolute age data in Table 1. New Zealand stages defined in Fig. 2. Revision of the Site 593 biostratigraphy now indicates an erosional unconformity exists at the top of the orange unit and contributes to the identification of the condensed section. See NOTE ADDED IN PROOF.

Miocene orange oxidised unit (418–393.8 mbsf; Leg 90 Shipboard Scientific Party 1986), which may be associated with intermediate waters that were sufficiently oxygenated to prevent post-depositional reduction within the sediments (Nelson 1986a), a suggestion supported by the foraminiferal assemblage (Boersma 1986). The presence of a thicker than normal (up to 6 m) surficial oxidised zone at the site reflects the presence of northward-flowing, oxygen-rich AAIW at core-top depth (Nelson 1986a).

The carbonate content of the Miocene and Pliocene sections exceeds 90% (Fig. 3A), but reduces to 75–90% in the late Pliocene–Holocene sections (Mycke et al. 1986; unpubl.

data). The persistently high carbonate content indicates the site has always been well above the regional lysocline and CCD, at c. 3600 and >4200 m depth, respectively (Kennett & von der Borch 1986a; Martínez 1994).

The non-carbonate component of the sediment consists mainly of clay minerals (Fig. 3B) with minor quartz, feldspar, pyrite, and glass shards (Nelson 1986a; Robert et al. 1986). The sources of this material include: (1) aeolian dust blown by the prevailing westerlies from Australia (Thiede 1979); (2) South Island (Southern Alps) derived clays delivered via ocean currents (Robert et al. 1986; Stein & Robert 1986); and (3) volcanic ash layers evident as thin, diagenetically altered pale green laminae (Gardner et al. 1986b), or as megascopic tephras (Nelson 1986a).

Age

The age structure for the Neogene interval of core is based on several key bioevents, as well as limited paleomagnetic and absolute age information (Table 1), documented elsewhere by

Table 1 Hole 593 stratigraphic tie-points and sedimentation rates used in this study.

Event	Depth (mbsf)	Age (Ma)	Sedimentation rate (m/m.y.)
Radiocarbon date (corrected)[a]	0.31	0.0159	19
FAD *Emiliania huxleyi*[a]	5.07	0.268	25
LAD *Pseudoemiliania lacunosa*[a]	9.91	0.458	20
Brunhes/Matuyama[b]	16.30	0.78	20
Top Jaramillo[b]	20.70	0.99	35
Base Jaramillo[b]	23.50	1.07	14
Top Olduvai[b]	33.33	1.77	10
Base Olduvai[b]	35.65	1.95	24
Isotope stage 100[c]	49.00	2.53	21
Isotope stage 104[c]	51.00	2.58	10
Base Gauss[b]	59.90	3.58	39
LO *Globorotalia punticulata*[d]	123.01	5.20	69
LO *Globorotalia sphericomiozea*[d]	143.69	5.50	34
FAD *Amaurolithus primus*[e]	203.42	7.24	34
HO *Bolboforma praeintermedia*[d]	236.42	8.21	100
LO *Bolboforma praeintermedia*[d]	240.42	8.25	13
HO *Bolboforma metzmacheri ornata*[d]	240.82	8.28	31
LO *Bolboforma metzmacheri ornata*[d]	246.17	8.45	24
HO *Bolboforma metzmacheri* ss. upper subzone[d]	254.19	8.78	6
HO *Globoquidrina dehiscens*[d]	254.30	8.80	31
Top Tukemokihi Coiling Zone[d]	269.07	9.27	44
Base Tukemokihi Coiling Zone[d]	270.82	9.31	34
LO *Bolboforma metzmacheri* s.s. upper subzone[d]	271.83	9.34	29
Bolboforma metzmacheri s.s. abundance spike[d]	274.70	9.44	21
LO *Bolboforma metzmacheri* ss. lower subzone[d]	276.82	9.54	26
HO *Bolboforma gracilireticulata* s.l.[d]	278.61	9.61	43
LO *Bolboforma gracilireticulata* s.l.[d]	284.62	9.75	8
HO *Bolboforma pentaspinosa*[d]	287.18	10.08	49
HO *Bolboforma capsula*[d]	289.69	10.13	40
LO *Bolboforma pentaspinosa*[d]	290.42	10.15	64
LO *Bolboforma capsula*[d]	293.61	10.20	13
HO *Bolboforma grüetzmacheri*[d]	295.01	10.31	27
LO *Bolboforma grüetzmacheri*[d]	299.02	10.46	139
HO *Bolboforma subfragoris* s.l. abundance spike[d]	304.57	10.50	21
Top Mapiri Coiling Zone[d]	306.02	10.57	21
Top Mapiri Coiling Zone[d]	306.65	10.60	18
Bolboforma subfragoris s.l. abundance spike[d]	306.83	10.61	11
Top Kaiti Coiling Zone[d]	309.05	10.82	56
Base Kaiti Coiling Zone[d]	315.25	10.93	31
FO *Bolboforma subfragoris* s.l.[d]	334.62	11.56	27
NN6/NN7 boundary[e]	341.16	11.80	34
Top *Bolboforma* sp. cf. *clodiusi Zone*[d]	376.65	12.83	8
LO *Orbulina suturalis* (popn)[d]	393.96	15.10	2
Globoconella miozea coiling transition[d]	395.82	16.06	7
FO *Globoconella miozea*[d]	406.65	17.60	14
FO *Globorotalia praescitula*[d]	426.10	19.00	

[a]From Nelson et al. (1986b) and Dudley & Nelson (1989).
[b]Paleomagnetic dates updated after Dudley & Nelson (1989), Berggren et al. (1995a,b)
[c]After Naish (1996), following Shackleton et al. (1995).
[d]Dates determined by Crundwell (2004).
[e]After Lohman (1986) and Raffi & Flores (1995).
LO = Lowest occurrence, HO = highest occurrence, FO = first occurrence; FAD = first appearance datum, LAD = last appearance datum.

Cooke (2002) and Crundwell (2004). The ages of the New Zealand Neogene stages, shown later alongside the textural records, are from Morgans et al. (1996). The database involves c. 1900 samples, providing a temporal resolution of 3–20 000 yr per sample over the 19 m.y. time span. Sedimentation rates generally range from 20 to 60 m/m.y. (Fig. 4), but drop to <10 m/m.y. over the interval between c. 18 and 14 Ma.

METHODS

Samples were dried, weighed, placed in pH 9.4 buffer solution (4 g $NaHCO_3$ + 1 g Na_2CO_3 in 20 *l* distilled water, as per Dudley & Nelson 1989), and left overnight. They were washed over a 63 µm sieve and the collected <63 µm mud fraction was allowed to settle and transferred into jars with buffer solution for storage. The >63 µm sand fraction was rinsed with distilled water and dried, then dry sieved into "fine" (63–150 µm) and "coarse" (>150 µm) sand fractions, weighed, and stored. Note that for the upper part of the record the boundary between fine and coarse sand was at 125 µm rather than 150 µm (e.g., Head & Nelson 1994; Nelson et al. 1994). The weight percent of coarse sand, fine sand, and mud was then derived for all samples.

Details of grain-size distribution within the mud fraction alone were made on a Malvern Lasersizer which incorporated a 300 RF lens, enabling size data to extend down to 0.05 µm. The size calculations used by the Lasersizer convert the particles to "equivalent spheres" (Rawle 1995), and for comparative purposes these have been extracted and grouped into nine grain-size classes ranging from coarse silt to very fine clay (Table 2). For a selection of mud samples from the late Miocene interval only, the graphical statistics of Folk & Ward (1957) have also been calculated. A qualitative assessment of the composition of selected samples was made using a binocular microscope for the sand fraction and the SEM for the mud fraction.

RESULTS

Bulk texture

A reference textural stratigraphy for coarse sand, fine sand, silt, and clay fractions is plotted against sub-bottom depth in Fig. 5. The same records versus age are shown in Fig. 6, both as raw and smoothed plots.

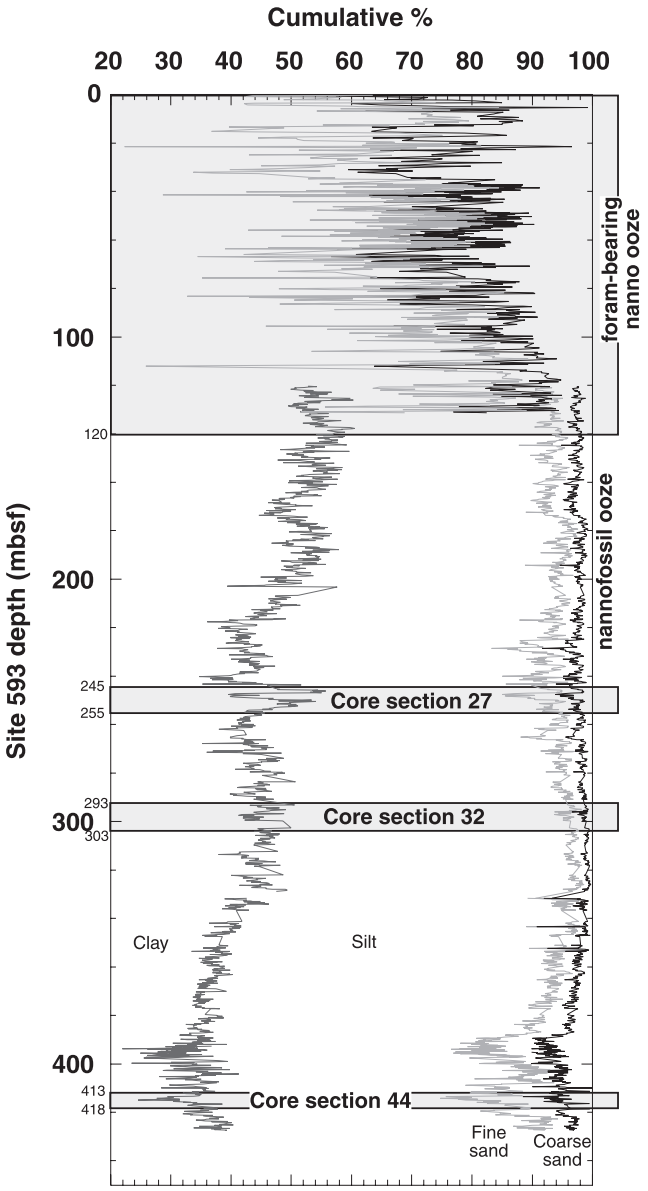

Fig. 5 Bulk texture data versus sub-bottom depth (metres below seafloor) from DSDP Hole 593. Grey boxes cover the intervals logged as foram-bearing nanno ooze, rather than simply nanno ooze, by the Leg 90 Shipboard Scientific Party (1986).

Table 2 Grain-size classes used in this study (after Folk 1968).

Grain size class	Abbreviation	Size (µm)	Size (ø)
Coarse sand	cs	>150 (125)	2–3
Fine sand	fs	150 (125)–63	3–4
Coarse silt	cz	63–31	4–5
Medium silt	mz	31–15.6	5–6
Fine silt	fz	15.6–7.8	6–7
Very fine silt	vfz	7.8–3.9	7–8
Very coarse clay	vcc	3.9–2	8–9
Coarse clay	cc	2–0.98	9–10
Medium clay	mc	0.98–0.49	10–11
Fine clay	fc	0.49–0.24	11–12
Very fine clay	vfc	<0.24	>12

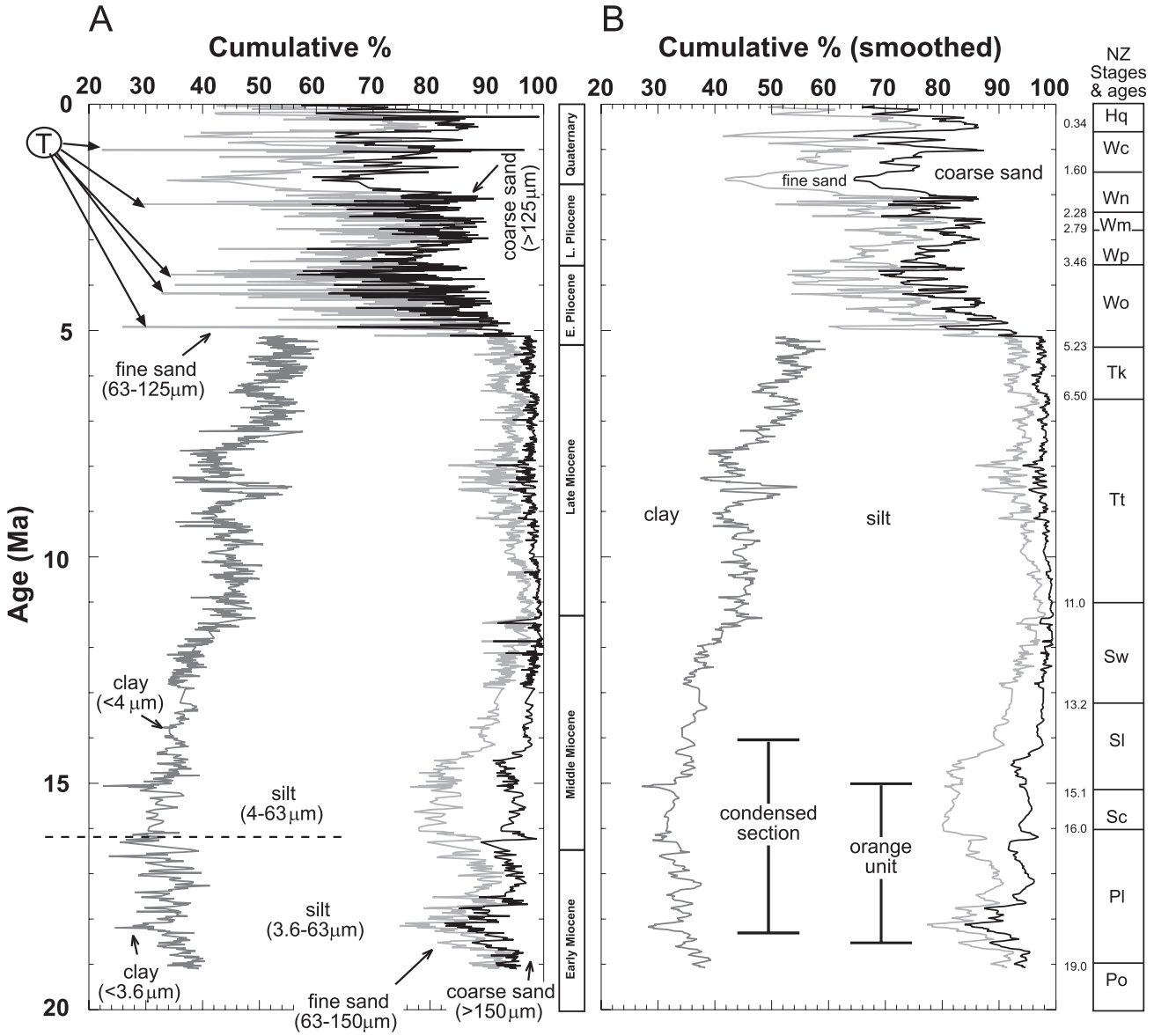

Fig. 6 Bulk texture versus age (Ma) from Hole 593: **A**, Cumulative percent; **B**, Cumulative percent smoothed using a five-point average generated from the software KaleidaGraph. The cumulative percent axes are shown down to 20% only. T = megascopic tephras which contribute to the increased sand content.

Sand

The total sand content is mainly c. <15% throughout the Miocene interval, except between 18.5–18.0 Ma and 16.5–14.5 Ma where it can exceed 20% (Fig. 6). In the Pliocene–Quaternary interval, sand contents are systematically much greater, reaching 50% or more in many samples. The intervals of increased sand content correspond reasonably well with the sections of Neogene core logged as foram-bearing nannofossil ooze by the Leg 90 Shipboard Scientific Party (1986), rather than the predominant nannofossil ooze (Fig. 5). In addition, the increased sand content through the Pliocene–Pleistocene interval corresponds with increased occurrence of tephric material over this time period (Fig. 6A) (Nelson et al. 1986a).

Mud

Mud sizes dominate all except a few of the Pliocene–Pleistocene samples, on average accounting for 85–95% of the Miocene interval, and 50–70% of the Pliocene–Quaternary interval (Fig. 6). Within the mud fraction, at least for the Miocene, there is an overall up-core increase in the content of clay compared to silt sizes, from typically 30–40% in the early part of the record to 50–60% by c. 5 Ma (Fig. 6). Noticeable features include the change in proportion of silt to clay from c. 16.5 to 15 Ma, and a 10% decrease in the silt fraction with a corresponding increase in clay fraction from 9 to 8.5 Ma, matching with the increase in sand content in core section 27 (Fig. 5).

Detailed mud analysis

Silt and clay classes

The dominant contribution of silt to the mud fraction occurs within the very fine silt class, followed by the fine silt class, so that the bulk of any changes in the content of silt in samples likely reside within these size intervals (Fig. 7). Likewise, the most abundant of the clay sizes is very coarse clay. Clays

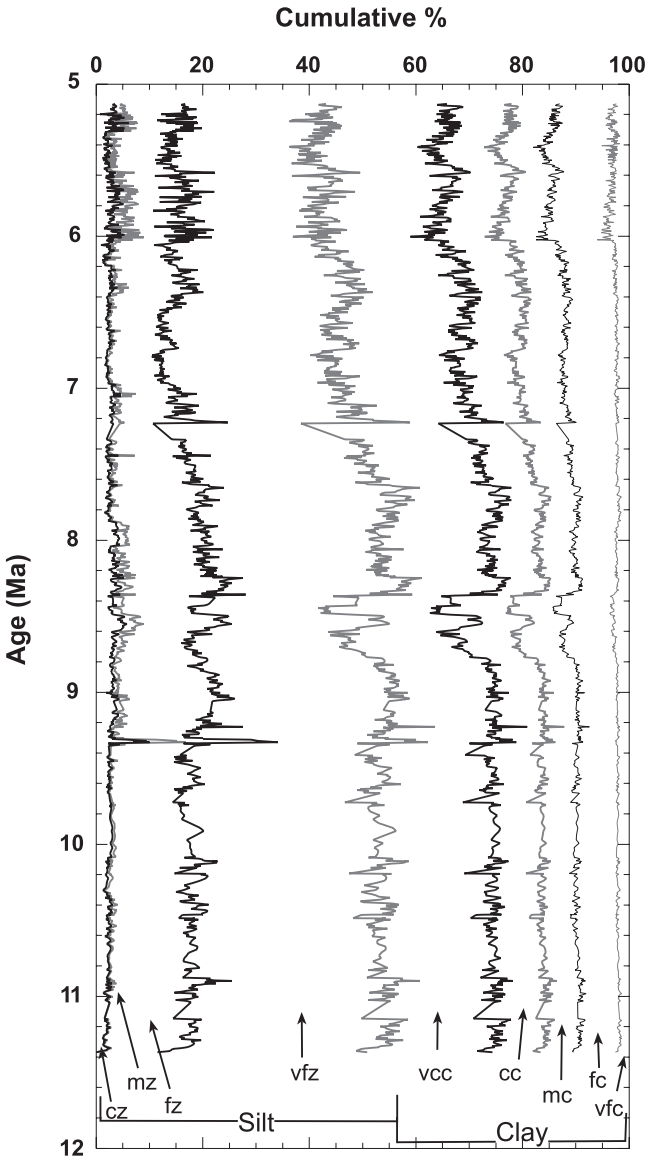

Fig. 7 Late Miocene Hole 593 mud fraction trends (divided into four silt 1 ø fractions, and five clay 1 ø fractions (see Table 2 for abbreviations). The dominant fraction is the very fine silt grade (7–8 ø, 7.8–3.9 μm).

increase significantly in content from 9 to 8.4 Ma (Fig. 7), and all clay divisions exhibit an up-core trend of increasing quantities after 8.4 Ma. This indicates either an increase in clay-sized grains or the removal of silt-size material, since all plots are proportioned to 100%.

Silt and clay divisions

The size data were analysed to see if the grain-size trends noted in the silt and clay data can be narrowed down to particular size ranges, with the intention of determining the composition of those sizes, and to apply grain-size statistics. These data (see Cooke 2002 for more detail) indicate that a grain population in the fine silt to very coarse clay size range (c. 13–3 μm) is absent/reduced in quantity, with grains larger and smaller remaining.

Mud grain-size statistics

Trends in grain-size parameters for the mud fraction over the late Miocene interval of core are shown in Fig. 8, and summarised in Table 3 (calculated in the standard phi format). Mean grain size shows a general up-core decrease from very coarse clay over the interval 11.5–7.5 Ma, to coarse clay through 7.5–5.0 Ma (Fig. 8A). Sorting generally becomes poorer up-core, with noticeable decreases between c. 9 and 8 Ma, and from 6 to 5 Ma (Fig. 8B). Most samples over the interval 11.5 through to c. 7.5 Ma are strongly fine-skewed (Fig. 8C), then there is an up-core trend for samples to become fine skewed, with a considerable number becoming near-symmetrical after 6 Ma. Kurtosis values are typically mesokurtic to leptokurtic (Fig. 8D).

Modality of mud fraction sizes

A consistent feature of the grain-size distributions within the mud fraction is the occurrence of three grain-size modes throughout the Neogene interval, but only studied in detail for the late Miocene interval (Fig. 9).

Coarse silt mode 4.25–4.75 ø (53–38 μm)

Although in very small quantities (0.3–2%), this coarse mode is consistently present in the mud fraction of all samples (Fig. 10A,B). There is a slight increase in the amount of material within the coarse silt mode from 9 and 8 Ma, and again between 6 and 5 Ma (Fig. 10B), with the older section not exhibiting any change in the modal grain size (Fig. 10A).

Table 3 Summary of range of grain-size statistics for the late Miocene mud fraction in comparison with Holocene core-top samples at Site 593.

Mean (ø)	Sorting (ø)	Skewness	Kurtosis
Late Miocene			
8.33–9.67 Very coarse to coarse clay	1.51–2.1 poorly to very poorly sorted	–0.07 to 0.8 near-symmetrical to strongly fine-skewed	0.68–1.49 platykurtic to very leptokurtic
Core-top			
8.33–9.33 Very coarse to coarse clay	1.66–2.81 poorly to very poorly sorted	–0.04 to 0.27 fine skewed to near-symmetrical	0.99–1.49 mesokurtic to leptokurtic

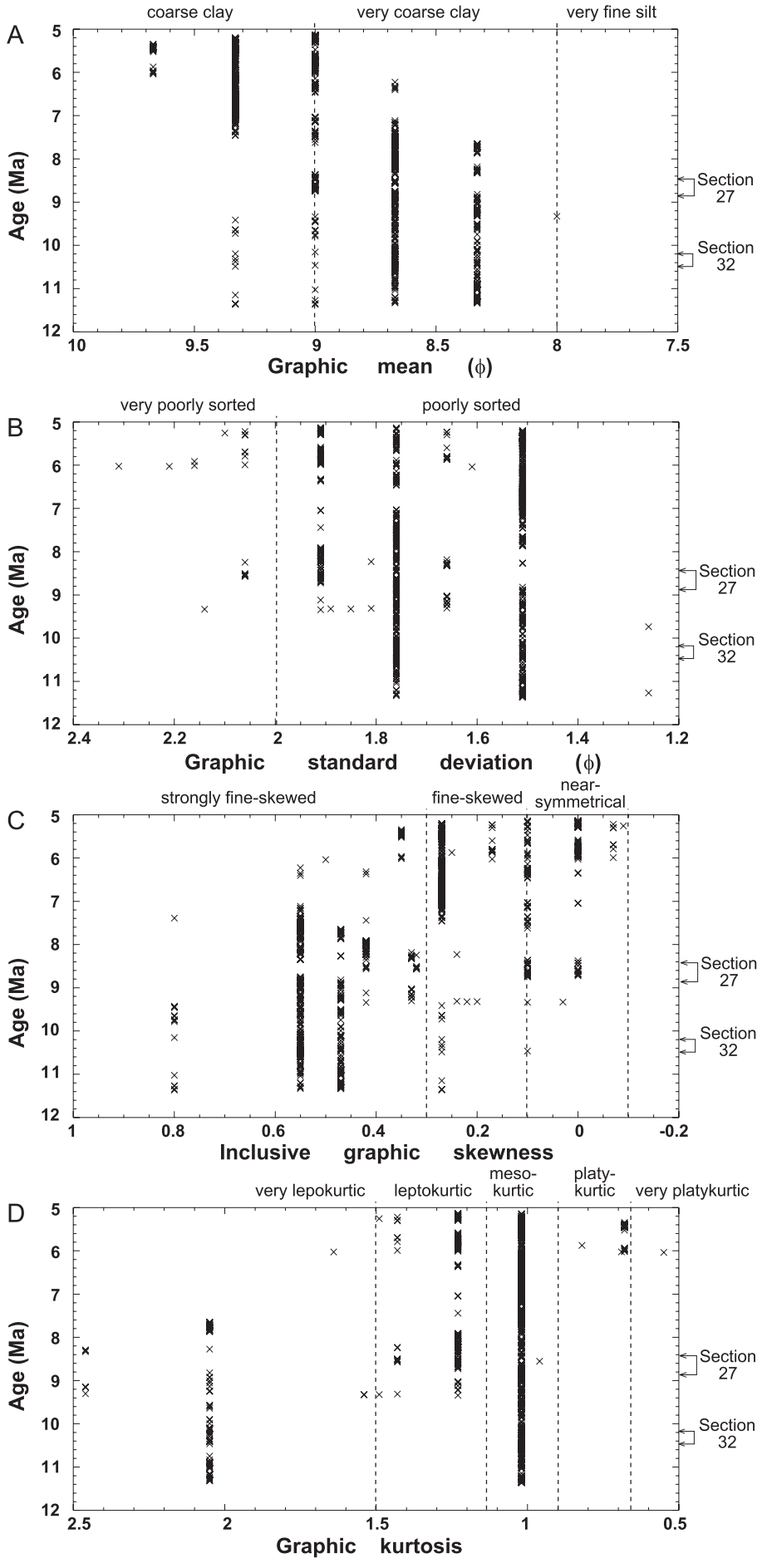

Fig. 8 Grain-size statistics for the late Miocene mud fraction from Hole 593 (using the 0.25 ø data detailed in Cooke 2002). **A**, Graphic mean (ø); **B**, Inclusive graphic standard deviation (ø); **C**, Inclusive graphic skewness; **D**, Graphic kurtosis. Sections 27 and 32 are noted.

Very fine silt mode 7.25–7.75 ϕ (6.6–4.7 μm)

This mode is the largest in quantity of the three (Fig. 10C, see also Fig. 9) and comprises 6–11% of the mud fraction (Fig. 10D). There is a general up-core decrease in the amount of the grains contributing to this mode with a noticeable decrease over the interval c. 8.9–8.5 Ma. The amount of material of this size increases from 8 to 7.5 Ma, co-incident with the modal size shift, but then decreases again until 6 Ma when there is a further reduction in the amount of material and the modal size decreases.

Fine clay mode 11.25–11.5 ϕ (0.41–0.35 μm)

This mode is consistently present in all samples (Fig. 10E, see also Fig. 9). It contributes c. 1.5–2.5% of the samples between 11.4 and 7.5 Ma, except for the section between 8.9 and 8.6 Ma where it increases to 3.2%, with further increases to as much as 4% of the total mud fraction by 5 Ma (Fig. 10F).

Grain size versus composition

Microscopy demonstrates that a general relationship exists between grain size and dominant grain composition (Table 4). Sand-sized material is composed mostly of foraminiferal tests, with minor bolboforms (Cooke et al. 2002), occasional glass shards, quartz, feldspar, and authigenic celestite and pyrite grains (Kennett & von der Borch 1986a; this study). The coarse silt fraction consists mainly of juvenile foraminifera with considerable amounts of broken test fragments, and minor amounts of glass shards. Most of the finer material comprises nannofossil placoliths of c. 3–6 μm size, while the smallest sizes (<3 μm) contain nannofossil placolith lathes, broken fragments of placoliths, and clay minerals (Fig. 11).

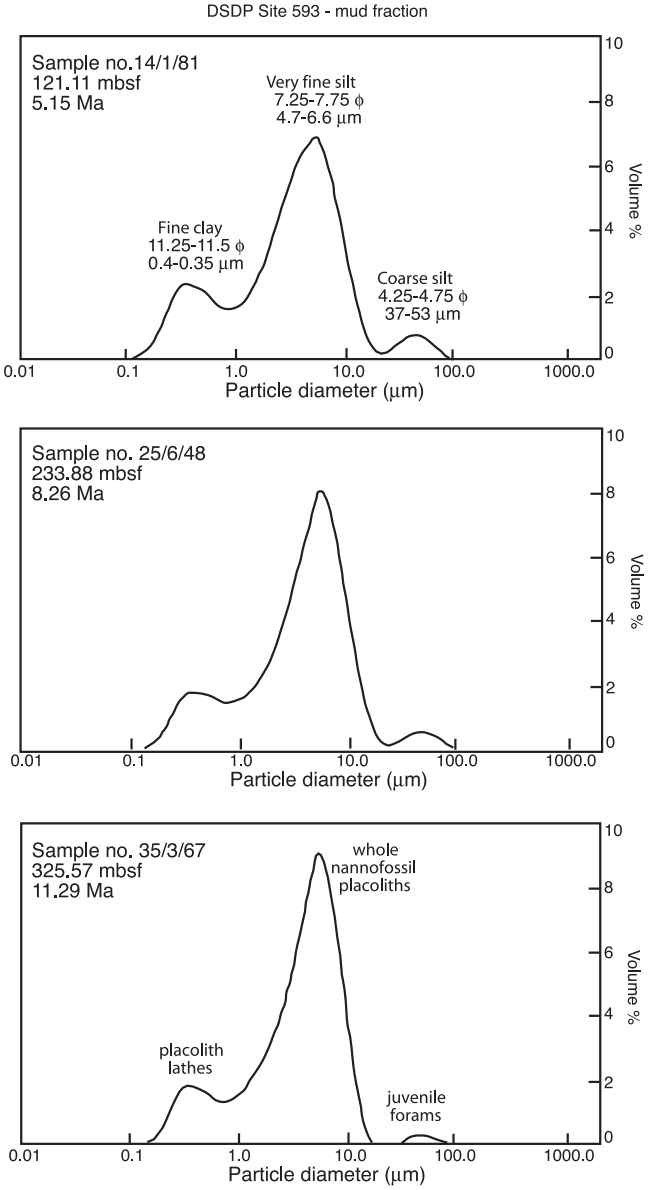

Fig. 9 Three samples illustrating the typical trimodal grain-size distribution in samples in the Hole 593 mud fraction. Fine clay mode, 0.35–0.4 μm; very fine silt mode, 4.7–6.6 μm; coarse silt mode, 37–53 μm. This trimodal pattern occurs throughout the entire study interval, c. 19–0 Ma.

DISCUSSION

Controls on sediment texture

Processes responsible for the supply of sediment, and those occurring after deposition, can affect sediment texture. These include organic productivity (Gorsline 1984), water column dissolution (Berger 1970; Berger & Winterer 1974), seafloor winnowing (Gardner et al. 1986a), sediment bioturbation (Nelson 1986a), and burial diagenesis (Garrison 1981).

Dissolution and diagenesis

Dissolution is discounted as having any major influence at Site 593, principally because the site lies well above both the lysocline (c. 3600 m) and the CCD (>4200 m) in the southern Tasman Sea (Martínez 1994), a situation that is assumed to have prevailed throughout the Neogene as carbonate contents are above 90% (Fig. 3A). The ooze/chalk transition at Site 593 occurs well below the Neogene interval analysed in this study (Nelson 1986a), so that the sediments

Table 4 Grain size versus composition of the Neogene Hole 593 sediments.

Composition	Sand	Coarse silt	Fine silt-clay	Clay
Detrital (<10%)	glass shards	glass shards	quartz/feldspar	clay minerals
Biologic (>90%)	adult forams, ostracods, bolboforms	juvenile forams, broken test fragments	placoliths (= coccoliths)	small placoliths, placolith fragments, micrite
Diagenetic	pyrite, celestite			micrite

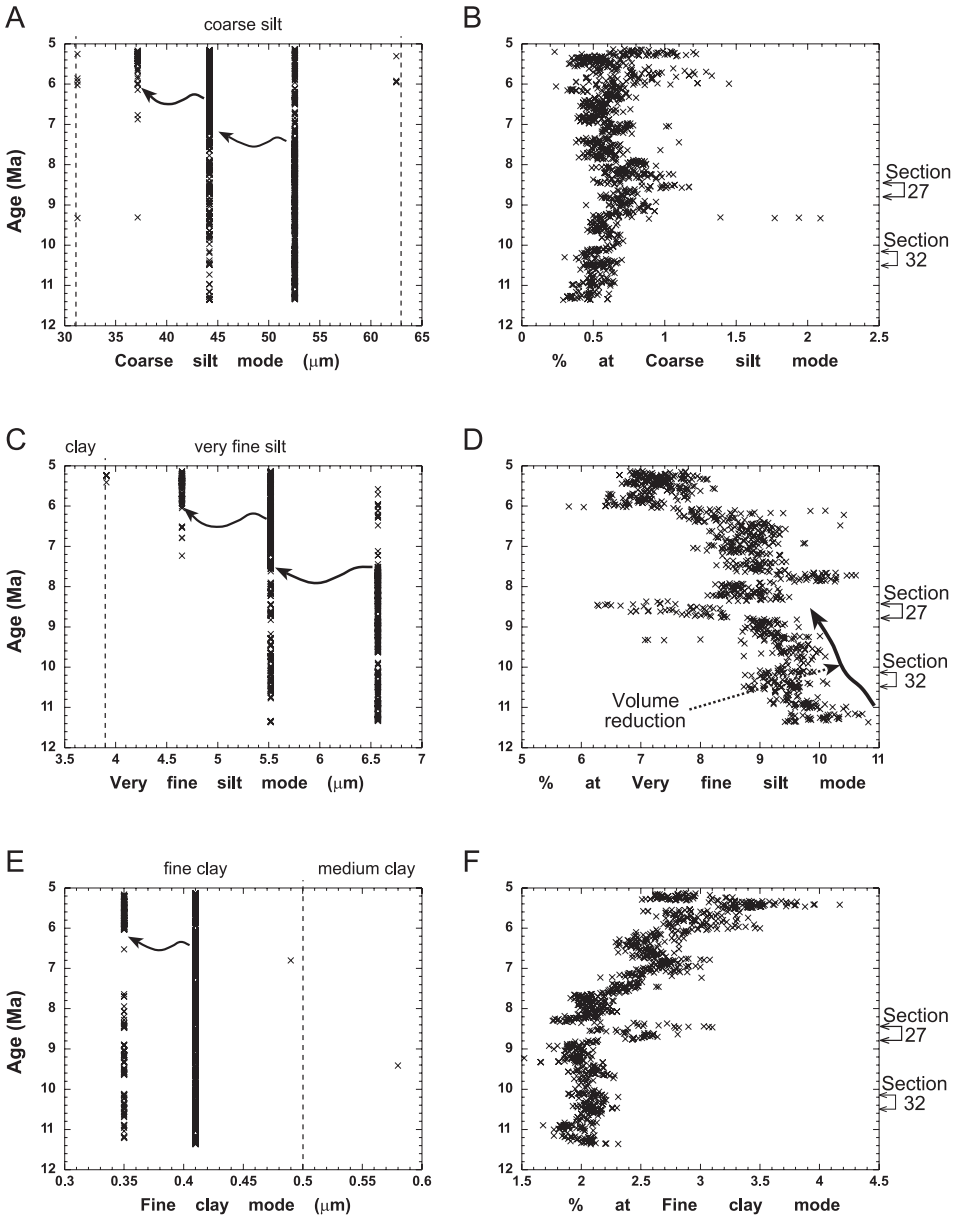

Fig. 10 Late Miocene mud fraction size and percentage of grains at each mode: **A, B** coarse silt mode; **C, D** very fine silt mode; **E, F** fine clay mode. Modal shifts are evident, for example, in (C) at 7.5 Ma where the dominant grain size of the very fine silt mode shifts from 6.6 to 5.5 μm.

are essentially unlithified (Fig. 2). The lack of cementation between nannofossil placoliths (Fig. 11A,C) also supports the inference that the Neogene Hole 593 oozes have not been subjected to significant dissolution and/or recrystallisation during burial. Shipboard studies on the Site 593 sediments showed that the foraminifera are well preserved throughout and that nannofossil preservation is generally good (Boersma 1986; Kennett & von der Borch 1986a; Nelson 1986a), opinions confirmed by our own SEM observations (Fig. 11). Nannofossil preservation can be used as an indicator of the degree of alteration and/or recrystallisation that has affected the sediment. For example, discoasters generally are the first group to show secondary overgrowths (Nelson 1986a), but such re-precipitation is rare on the discoasters imaged in this study (Fig. 11B–D). What is sometimes evident on the discoaster nannoliths is post-depositional pressure dissolution (Fig. 11B–D) with the imprinting of reticulofenestrid placoliths on the surface (e.g., Fig. 11D). Occasional evidence of placoliths cementing to ostracod carapaces (Fig. 11E,F) could be the result of recrystallisation of the ostracod calcite, rather than the dissolution of nannofossil calcite. While ostracods from Tasman Sea sites nearer to New Zealand do show signs of dissolution (Swanson & van der Lingen 1997), these sites are influenced by "coastal" upwelling systems (Bradford & Roberts 1978). Although ostracods are more prone to dissolution than foraminifera (Swanson & van der Lingen 1997), they only contribute in minor quantities to the sand fraction in Hole 593, and any dissolution is considered to have had a minor effect on the grain-size variations reported here.

Bioturbation

While burrowing and vertical mixing of sediment will destroy any stratigraphic changes in grain size, bioturbation within the Neogene section of Hole 593 is uniformly low (Nelson 1986a). The two most important factors influencing bioturbation are sedimentation rate and organic nutrient supply to the seafloor (Nelson 1986a). Since the sedimentation

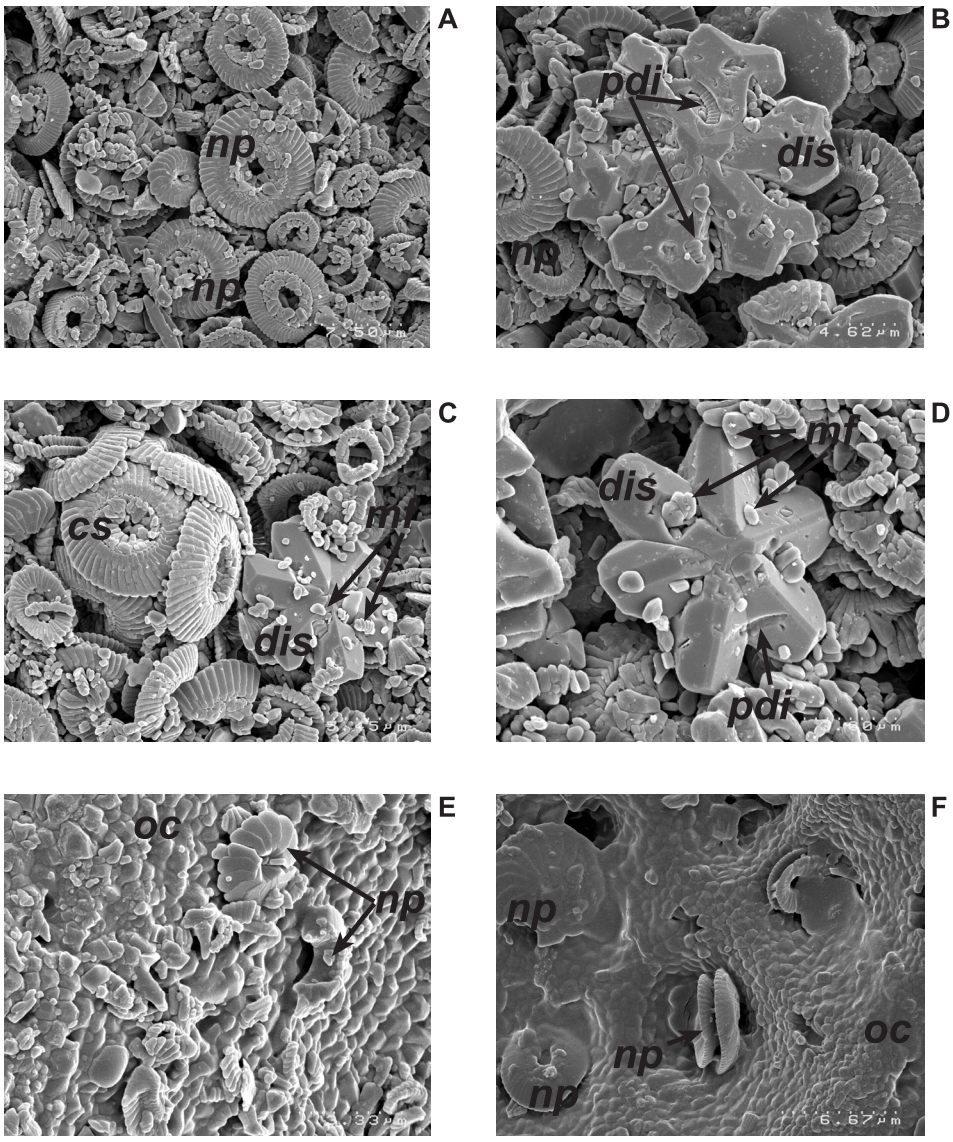

Fig. 11 SEM images of the mud fraction from Hole 593 with the scale on the bottom right-hand corner. **A**, 90-593-42-5, 130—nannofossil placoliths (= *np*). **B**, 90-593-43-4, 48—discoaster (= *dis*) exhibiting pressure dissolution imprints (= *pdi*) from placoliths. **C**, 90-593-43-5, 22—whole coccosphere (= *cs*) and discoaster (= *dis*) with micrite fragments (= *mf*). **D**, 90-593-44-2, 71—discoaster with micrite fragments and some pressure dissolution imprints. **E**, **F** 90-593-12-1, 69 (E) and 90-593-32-4, 30 (F)—ostracod carapaces (= *oc*) on to which individual placoliths have become cemented.

rate at the site has been relatively uniform (Fig. 4), it is unlikely to have dramatically affected the extent of bioturbation. Site 593 is presently located within an oligotrophic part of the Tasman Sea unaffected by upwelling that could contribute large amounts of organic material to the seafloor (Bradford & Roberts 1978). The site is located within either the lowest or second lowest productivity categories determined by Bradford & Roberts (1978) for the southern Tasman Sea, and there is little to indicate significant change in this situation through the Neogene. Hence, by assuming similar oligotrophic conditions in the past, this might help explain the relatively low degree of bioturbation of the sediments.

Productivity

Changes in biological productivity may alter the sediment texture due to succession in the dominant organism(s) in the overlying ocean waters. The carbonate biogenic contributors to Hole 593 sediments are nannofossils (majority), then foraminifera, and finally minor amounts of ostracods and bolboforms (Table 4). Sites c. 150 km offshore do record changes in paleoproductivity with carbonate contents ranging between 33 and 66% (Swanson & van der Lingen 1997), but these may be subject to localised upwelling (Bradford & Roberts 1978). While intermittent upwelling along the South Island West Coast is evident in the modern coastal system (Vincent & Howard-Williams 1991), these colder water plumes are transient, only extend up to 75 km offshore (versus Site 593 at 270 km offshore), and are in part related to riverine discharge along the coast. Hence, any contribution to increased paleoproductivity that upwelling might make is unlikely to have affected Site 593 to any great extent.

In regions of high primary productivity in the vicinity of upwelling or oceanographic fronts, the flux of phytoplankton will be higher than in more oligotrophic areas (Yoder et al. 1994; Murphy et al. 2001), which would alter the ratio of nannofossils to foraminifera (Gasol et al. 1997). Site 593 is not presently located near an oceanographic front, nor has it done so in the past (Nelson & Cooke 2001). As the only biological material accumulated at Site 593 is calcareous (Caulet 1986), the total phytoplankton contribution to the system cannot be established (any diatoms may have been dissolved at the seafloor by the silica-undersaturated AAIW/SCIW). To estimate the foraminifera:nannofossil ratio, mass accumulation rate (MAR) data are needed. These are not

available for Site 593 but have been calculated by Gardner et al. (1986a) for Site 591 to the north (Fig. 1). Although the late Miocene sedimentation rates at Site 593 (Fig. 4) are slightly higher (c. 20–60 m/m.y.) than at Site 591 (c. 20 m/m.y.), both sites have similar late Miocene sand:mud ratios of c. 10:90, interpreted as reflecting similar paleoproductivity rates. Early late Miocene sedimentation rates at Site 591 are similar to those occurring on carbonate platforms outside regions of high paleoproductivity, and the MARs are typical of the Southwest Pacific at this time (Gardner et al. 1986a). If the assumption is made that all the coarse fraction (>63 μm) and 10% of the fine fraction (<63 μm) comprises foraminifera, and the remaining fine fraction is nannofossils, Site 591 has a foraminifera:nannofossil ratio of 15:85, even though it is closer to the high productivity region associated with the Tasman Front (Gardner et al. 1986a). If similar reasoning is applied to Site 593, where the coarse fraction rarely exceeds 10% through the middle–late Miocene, and there is a small contribution of juvenile foraminifera (say, c. 5%) to the mud fraction, a comparable ratio is determined. In Hole 591 the MARs increase through the latest Miocene into the Pliocene, and are interpreted as the result of increased paleoproductivity associated with upwelling along the Tasman Front (Gardner et al. 1986a). As there is no corresponding change in the foraminifera:nannofossil ratio in Hole 593, we infer that Site 593 has not been subjected to large-scale fluctuations in paleoproductivity.

Changes in the amount of dissolved CO_2 in the sea water around Site 593 could have an impact on carbonate dissolution. However, the alkalinity of the sea water (i.e., the concentration of hydrogen carbonate and carbonate ions—which is not a measure of sea water pH nor how alkaline the water is; Varney 1996) of the Tasman Sea will be affected by the amount of biological activity (much of which cannot be accounted for, such as bacteria and viruses which are not preserved in the sediments) and its subsequent metabolic production of CO_2. Hence, any assumptions regarding dissolution in the Neogene Tasman Sea have this caveat.

Winnowing

Winnowing typically involves the selective erosion and transport of certain fine fraction components, or the selective non-deposition of that fine fraction, leaving the coarse fraction relatively intact. The extent of any winnowing depends on sediment composition and bottom water velocity, and may change in the course of time with formation of a surficial lag deposit of coarser material that shields the underlying sediments from further erosion (van Andel 1973; Jenkins 1985, 1992). Having discounted factors such as dissolution, bioturbation, diagenesis, and large-scale paleoproductivity changes to explain the textural changes at Site 593, it remains that fluctuations in the sand:mud ratio likely result from one, or some combination, of the following: (1) fluctuations in the amount of winnowing of mud from the sediments at the site; and/or (2) fluctuations in the amount of mud-sized sediment deposition, winnowed from up-current.

Site 593 is unlikely to have been a depocentre for mud winnowed from up-current as it is located near the top of the eastern slope of Bellona Trough on the western margin of Challenger Plateau (Fig. 1B) and, if anything, is more likely to be a site of sediment removal. Lack of any noticeable hiatuses within the Neogene sequence (Kennett & von der Borch 1986b; Nelson 1986b) suggests, however, that wholesale removal of sediment, for example by slumping or scour, has not occurred. Thus, changes in the sand:mud ratio are most likely a result of winnowing of mud from the bottom sediments, and possibly small-scale changes in paleoproductivity.

The long-term, up-core increase in the sand content at Site 593 is interpreted as progressive removal of increasing amounts of the mud fraction through the Neogene, with extreme winnowing beyond the general trend evident in the more notable increases in sand content between c. 19–17.5 Ma, c. 16.5–14.5 Ma, c. 9.5–8 Ma, and <5 Ma (Fig. 6B). The increased sand content from c. 16.5 to 14.5 Ma coincides with a condensed interval based on the biostratigraphy and sedimentation rates (Fig. 4) (Elkington et al. 2000), consistent with bottom sediment winnowing. The general up-core decrease in the fine silt to coarse clay fraction through the late Miocene (Fig. 7) is interpreted as winnowing because it demonstrates the removal of a particular size range, and because up to c. 40% of the mud fraction is finer than very coarse clay but is not being removed. That is, a specific size range is being picked out of the sediment, which implies a slight increase in water velocity, or perhaps pulsing of the water flow. The decrease in the amount of material in the very fine silt mode (Fig. 10D) over the interval 8.9–8.5 Ma and at 7.5 Ma also supports winnowing because the modal grain size does not change but the number of grains at that mode does. This mode comprises nannofossil placoliths, and so it must be these components that are being winnowed. If this change in volume was the result of large-scale paleoproductivity changes, all grain-size components linked to the nannofossils (including the smaller fragments) would be expected to change, not just the size range specific to the whole placoliths.

Since nannofossil placoliths do not develop the cohesive charges typical of fine terrigenous grains, the silt-cohesive boundary at 10 μm identified in terrigenous sediments (e.g., McCave et al. 1995) probably does not apply to calcareous oozes. The trend towards mesokurtosis is taken to indicate the persistent loss of the subsidiary grain-size population, in the fine silt to very coarse clay (c. 13–3 μm) size range (Fig. 8D). This is supported by the changes in skewness (Fig. 8C) where the loss of the fine tail from 9 to 8 Ma, and after c. 7.5 Ma, also indicates removal of a population of grains. This loss of fines is also evident in the up-core trend to reduced mean grain size, from very coarse clay (c. 3 μm) to coarse clay (c. 1.2 μm) (Fig. 8A). As the winnowed grains are removed and the grain population size changed, the sorting would be expected to deteriorate. It does so, with the grains becoming more poorly sorted over the interval c. 9–8.5 Ma, and again after c. 6.5 Ma (Fig. 8B).

From the above we infer that the major control on the sand:mud ratio at Site 593 is the velocity of the bottom watermass bathing the site, and any changes in it. The modern bottom water at the site is AAIW, and we link the textural fluctuations to changes in the strength of its Neogene equivalent, SCIW (Kennett & von der Borch 1986a; Flower & Kennett 1995). The velocity of AAIW is poorly known. Mean speeds of 2–8 cm/s at 1000 m depth are reported from the Tasman Sea and south of the Chatham Rise (Reid 1986; Hamilton 1990), while flow rates in the southern Indian Ocean above 2500 m depth, which include AAIW, are generally <10 cm/s (Park et al. 1993). So a velocity of c. 5 cm/s, certainly <10 cm/s, is assumed for the AAIW/SCIW watermass.

Southard et al. (1971) showed that currents in the 15–35 cm/s velocity range erode silt-sized foraminiferal tests

from the sediment surface. Since most of the silt-sized grains at Site 593 are nannofossil placoliths and not foraminiferal tests, it is likely that this overestimates the velocity needed to winnow the placoliths as they are smaller and have a hydrodynamically sensitive, plate-like morphology (Fig. 11). Silt-sized siliciclastic particles can be kept in suspension by currents faster than 1 cm/s and eroded by current velocities in the range of 6–15 cm/s (Ellwood & Ledbetter 1977). This suggests that changes in quantity of parts of the calcareous silt-size fraction ought to be sensitive enough to monitor bottom current velocity fluctuations in the Tasman Sea. In siliciclastic sediments, changes in bottom current speed below a scour-indicating velocity can be inferred from variations in the percentage of the 10–63 μm fraction (Huang & Watkins 1977). However, in some studies (e.g., Robinson & McCave 1994; McCave et al. 1995; Manighetti & McCave 1995), the siliciclastic fine fraction behaviour is dominantly cohesive below 10 μm and non-cohesive above that size, so that the silt fraction finer than 10 μm may behave like the clay-sized (<2 μm) fraction. Other studies do not record this silt-cohesive boundary (e.g., Howe & Pudsey 1999). Since the Neogene Site 593 sediments are carbonate dominated, the 10 μm cohesive boundary is unlikely to apply.

Mud size modes and composition

The dominant mud fraction in Site 593 sediments comprises three modes: coarse silt, very fine silt, and fine clay (Fig. 9). The coarse silt mode at 37–53 μm is mainly composed of whole juvenile foraminifera with a minor contribution from volcanic glass and aeolian dust (Table 4). The glass contribution is evident in the altered smectite clays (Gardner et al. 1986b). Aeolian material is evident in the Quaternary Tasman Basin sediments, which is consistent with the modern, predominantly westerly wind system blowing dust across the Tasman Sea from southern Australia (Hesse 1994). Dust has been reported on South Island snowfields with a size peak at c. 40 μm (Marshall & Kidson 1929; Windom 1969). The very fine silt mode comprises nannofossil placoliths, with the population dominated by the reticulofenestrid group (Lohman 1986). This group consists of an elliptical placolith with a central area that is either open or bridged by many small laths that form a reticulum (Fig. 11), hence the name, with placoliths ranging in size from <5 μm to large plates >7 μm (Young 1990; Takayama 1993). Particles contributing to the fine clay mode comprise reticulofenestrid-placolith fragments and micrometre-sized carbonate material, or micrite (Fig. 11). Minor amounts of smectite and illite (Robert et al. 1986) may also contribute to this mode.

Mud size mode shifts

The dominant grain size of the coarse silt mode shifts at c. 7.5 Ma from 52.6 to 44.2 μm, and shifts again at c. 6 Ma to 37.2 μm, suggesting that either the water velocity increased sufficiently to remove juvenile tests of c. 52 μm size, pushing the mode to a smaller size, or that the production of the tests was somehow changed, and the population test size of the juveniles got smaller. An increase in water velocity sufficient to remove coarse silt (38–63 μm) is likely to remove smaller sizes as well, and to produce sediment scour and hiatuses, for which there is no evidence. Therefore, the coarse silt modal shift is more likely to result from changes in foraminiferal paleoproductivity, either a general reduction in the size of the juveniles or a change in the dominant species contributing the juveniles. The position of this modal change at c. 7.5 Ma lies within the dominant shift in the silt/clay proportions (increasing clay) (Fig. 6B). This mode shift also corresponds with a decrease in foraminiferal diversity (M. Crundwell pers. data) and therefore most likely reflects a change in the species contributing to the mode. The very fine silt modal shift observed in the nannofossils occurs at the same horizon, which suggests that both shifts may be linked to small-scale surface water paleoproductivity changes, as all of the modes comprise <10% of the mud fraction (Fig. 9). Stabilisation of the position of both the Subtropical and Tasman Fronts, resulting in greater compartmentalisation of the Tasman Sea surface waters, may be a contributing factor (e.g., Nelson & Cooke 2001).

The very fine silt modal size shift occurs near c. 7.5 Ma (Fig. 10C), and since this mode is composed of nannofossils, variation within this group is further considered (bearing in mind the limited dating constraints). Significant changes in the size of reticulofenestrid placoliths (the dominant group at Site 593) during the middle–late Miocene have been reported in Atlantic and Mediterranean drill sites, with an increase in the numbers of small placoliths prior to FAD *Amaurolithus primus* at 7.24 Ma being noted (Flores & Sierro 1989; Flores et al. 1992). Young (1990) reported something similar at Indian Ocean sites, where the large (>7 μm) *Reticulofenestra pseudoumblilicus* disappears, resulting in a "small *Reticulofenestra* interval" which first appears in late NN10 (the NN10/11 boundary = 8.6 Ma). Between late NN11 and NN15 (top of NN11 at 5.6 Ma) the reticulofenestrid assemblage is strongly skewed towards smaller (<5 μm) placoliths. The *Reticulofenestra pseudoumblilicus* absence interval has also been documented in the equatorial eastern Pacific from 8.85 to 6.8 Ma (Raffi & Flores 1995). Clearly there is a biostratigraphic event involving size reduction, but it appears to be slightly diachronous between oceans, ending somewhere between 6.8 and 5.6 Ma. The explanations for this event include genotypic with ecological influences (Young 1990) and/or oceanographic-climatic instability (Rio et al. 1990).

At Site 593 the shift in the very fine silt mode from 6.6 to 5.5 μm at c. 7.5 Ma (Fig. 10C) reflects a change in the size of the grains (nanno placoliths) contributing to the mode. The second shift at 6 Ma is also inferred to reflect a further reduction in the size of the placoliths. But the size change needs to be distinguished from the effects of winnowing. Winnowing of sediment is inferred because grains from 13–3 μm size have been removed, leaving both larger and smaller grains in the samples. However, if the contributing placolith size became smaller then this would also result in a similar pattern, since grains of this size range (13–3 μm) would no longer be contributing to the sediment. Distinguishing between these two options is possible using the grain size of the very fine silt mode (Fig. 10C,D). While the proportional contribution of this mode reduces between 12 and 8 Ma (Fig. 10D), the actual size of this mode does not (Fig. 10C), indicating that grains contributing to the mode did not get smaller in size; there were just less of them. Therefore, because this modal size does not reduce during the time when *Reticulofenestra* placoliths reduce in size, the changes in sediment texture of the bioevent interval are inferred to be due to winnowing and not to a size reduction of the reticulofenestrids. However, at c. 7.5 Ma, the modal size shifts at a time when the proportion of grains stays reasonably

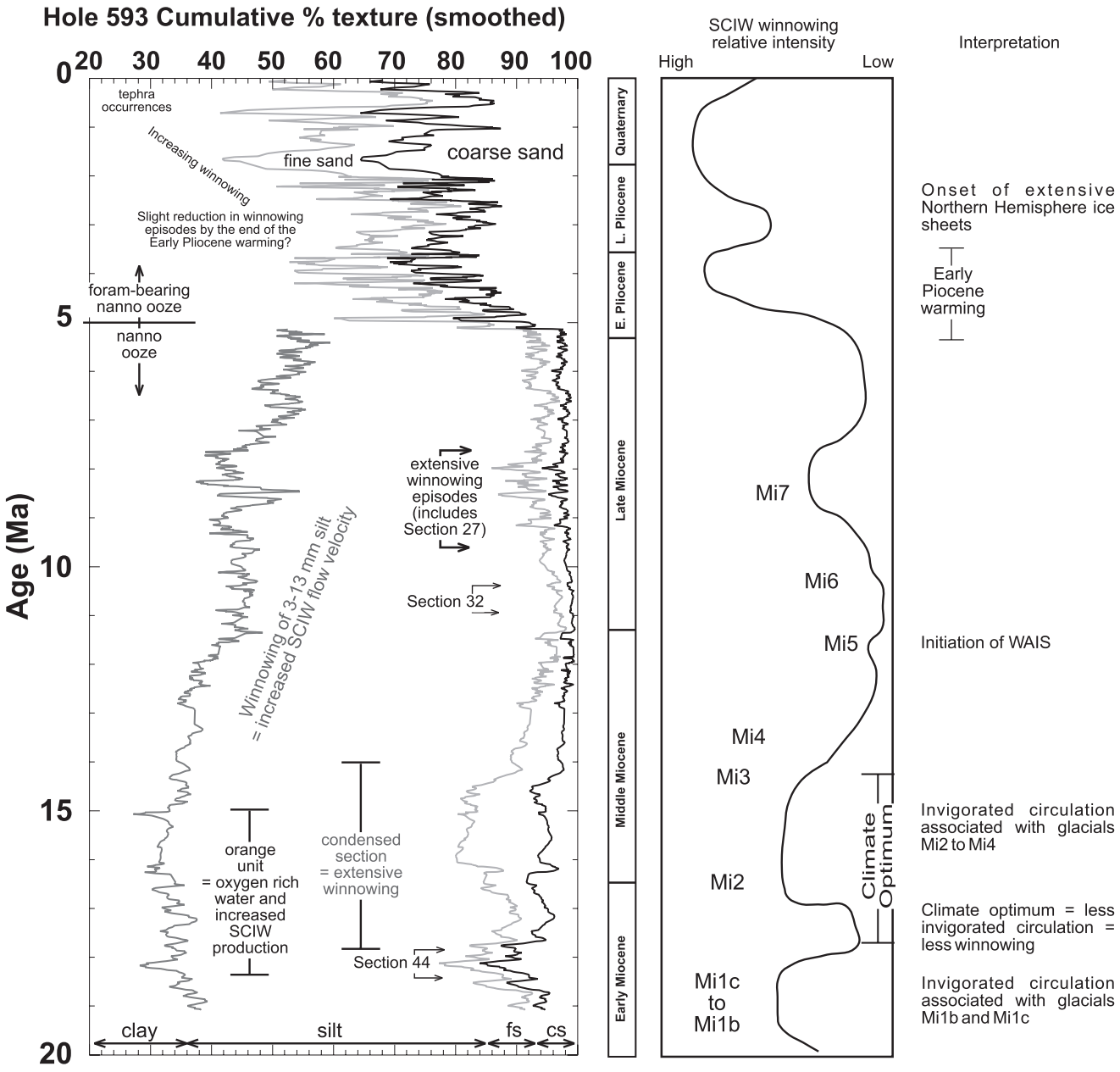

Fig. 12 Cumulative texture curves (from Fig. 6B) in relation to inferred winnowing intensity of Southern Component Intermediate Water (SCIW) throughout the Neogene at Site 593, southern Tasman Sea. Notable winnowing periods correspond with the condensed section (c. 18–14 Ma), core section 27 (8.42–8.83 Ma), the Miocene glacial zones (Mi1–Mi7), and the increasing ice volume associated with Northern Hemisphere ice sheet development after c. 4 Ma. Note the relative drop in winnowing intensity during the initial phase of the Miocene Climate Optimum, and also at end of the early Pliocene warming phase. Increased winnowing fluctuations follow from 2.5 to 0 Ma.

consistent (or even increases), and may indicate a reduction in the *Reticulofenestra* placoliths contributing to this mode. The textural changes over the interval 6–5 Ma, which have been inferred to be due to winnowing, might also have a component of reticulofenestrid placolith size reduction as the mean grain size reduces, along with the very fine silt mode shifting to 4.7 µm. Without detailed analysis of the nannofossil assemblage it is not possible to be more definitive, but we predict that the size of the mode should increase after the end of the "small *Reticulofenestra* interval".

Paleoceanographic interpretations

A general up-core decrease in the abundance of fine silt to very coarse clay sizes in the Neogene mud fraction from Hole 593 is inferred to be linked to an increase in flow velocity of the SCIW in the Tasman Sea (Fig. 12). The large increases in sand content (and reduction in silt) over the intervals c. 19–17.5 Ma, 16.5–14.5 Ma, 9.35–7.9 Ma, and after 5 Ma are taken to indicate especially invigorated SCIW circulation in the southern Tasman Sea. Most of the detailed textural data exhibit substantive changes from 8.8 to 8.4 Ma

(Section 27) (Fig. 8, 10), and a conspicuous increase in sand content over the interval c. 19–14.5 Ma (Fig. 6B) suggests these time intervals represent periods of accentuated current activity. If a modern flow velocity of c. 5 cm/s is assumed for AAIW, then faster speeds must have characterised its SCIW predecessor during winnowing events. However, for the pelagic ooze to accumulate as completely as it has on the Challenger Plateau (with the exception of the condensed section), persistently strong SCIW flow can be ruled out. Consequently, the subtle changes in the <63 μm mud grain-size data recorded during the late Miocene (Fig. 12) are inferred to define an overall increase in SCIW velocity. However, this did not reach as high as 15 cm/s, the velocity at which silt-sized foraminiferal tests are removed (e.g., Southard et al. 1971), because silt-sized foraminifera are consistently present in approximately the same proportions (1–5%) in samples. Conversely, increases in the amount of mud-sized material can be used as a proxy for reduction in SCIW velocity (Fig. 12). After c. 8 Ma it is concluded that while the current velocity decreased somewhat, it remained higher than before c. 9.5 Ma, because the percent mud is less after c. 8 Ma. From c. 5 Ma to the core top, the sediments are foram-bearing nannofossil ooze (Fig. 2) (Leg 90 Shipboard Scientific Party 1986), taken to indicate a continuation of winnowing through to the Holocene.

The intensification of the current speed of SCIW (AAIW) is linked to the oceanographic front which generates it, namely the Antarctic Polar Front (AAPF; Fig. 1). The position of the AAPF south of New Zealand is closely linked to the Australian-Pacific ocean spreading ridge (Nelson & Cooke 2001) and the wind speed of the polar westerlies (Perry & Walker 1977). The establishment of the West Antarctic Ice Sheet (WAIS) between 10 and 8 Ma (Ciesielski et al. 1982; Kennett & von der Borch 1986a) resulted in the meridional thermal gradient increasing, which in turn increased the volume of the middle–late Miocene SCIW (Flower & Kennett 1995). General changes in Pacific Ocean circulation intensity between 10 and 8 Ma have been inferred from fluxes in the biogenic opal record, which supports intensification in the Southern Hemisphere trade winds and equatorial upwelling (Leinen 1979). Tectonic collision significantly restricted the Indonesian Gateway between 16 and 12 Ma, resulting in intensification of the East Australian Current (Kennett et al. 1985), and the deep-water closure of the Panama Gateway by c. 10 Ma (Lyle et al. 1995; Collins et al. 1996) effectively initiated close to modern circulation patterns in the Pacific Ocean.

An increase in the >63 μm fraction at c. 10 Ma is evident in the sediments from Broken Ridge in the southern Indian Ocean and is attributed to an increase in winnowing energy associated with invigorated SCIW (House et al. 1991). These authors make the suggestion that the oxygen isotope evidence for an increase in ice volume at 13 Ma (i.e., glacial events Mi3 and Mi4; Flower & Kennett 1994, 1995) is manifested in the textural record at Broken Ridge some 3 m.y. after the ice effect. Significant regional cooling in the Southern Ocean at c. 9 Ma is also evident in the increase in ice-rafted debris at Kerguelen Plateau sites, associated with more extensive sea ice development (Bohrmann & Ehrmann 1991; Schlich & Wise 1992).

The increased winnowing at c. 9.5–8 Ma in Hole 593 sediments could reflect a similar delay between ice volume increase and oceanic changes in the Tasman Sea, a consequence of the middle–late Miocene isotope events identified in the oxygen isotope record from the region (Flower & Kennett 1995; Cooke 2002). Miocene glacial events Mi5 and Mi6 (c. 11.5–10.4 Ma) are interpreted as significant ice volume increases contributing to the development of the West Antarctic Ice Sheet (WAIS). If the winnowing in Hole 593 is attributed to Mi5 and Mi6, rather than Mi3/Mi4, then the delay reduces to no more than 2 m.y. The decrease in winnowing, and by inference reduction of SCIW velocity from c. 17.5 to 16.5 Ma in Hole 593 (Fig. 12), coincides with initiation of the late early Miocene climate optimum, a period of climate warming and less vigorous oceanic circulation (Woodruff & Savin 1991; Wright & Miller 1992). The decrease in mud content starting at c. 16.5 Ma, interpreted as increasing SCIW velocity, coincides with glacial zone Mi2 (16.1 Ma). Glacials Mi3 and Mi4 (c. 14–12.6 Ma), described as significant ice volume events (Miller et al. 1991; Flower & Kennett 1995), occur over an interval when the Hole 593 mud content increases. After c. 12.8 Ma the silt-sized component of the mud fraction starts to decrease, interpreted as increased winnowing following glacial events Mi3 and Mi4. This is inferred to reflect a reduced ice volume/oceanic effect delay during the early–middle Miocene in the Tasman Sea.

In Hole 593, increased winnowing is evident again after c. 7.5 Ma as this part of the core has the lowest silt content of the whole record (Fig. 12), and may reflect an ice volume/oceanic effect delay associated with Mi7 (c. 9.3 Ma). The increased winnowing occurs just before the FAD of *Amaurolithus primus* (Lohman 1986), a bioevent associated with the well-known Chron 6 Messinian Carbon Shift reported to be isochronous in the Atlantic and Pacific Oceans between 6.1 and 5.9 Ma (Keigwin & Shackleton 1980; Vincent et al. 1980; Hodell et al. 1986). The carbon shift occurs at, or immediately after, the FAD of *Amaurolithus* spp. (Haq et al. 1980), dated at 7.24 Ma in the Pacific (Berggren et al. 1995a; Raffi & Flores 1995), but 7.38 Ma in the Atlantic (Backman & Raffi 1997). Therefore, the age of the carbon shift is taken to be slightly younger than 7.24 Ma in Hole 593. The carbon shift is linked to climate cooling and oceanic reorganisation associated with the initiation of the Messinian Salinity Crisis (Shackleton & Kennett 1975; Elmstrom & Kennett 1986; Hodell et al. 1986). The Messinian crisis is now thought to record some sea-level lowering due to glaciation, in addition to a regional tectonic control (Blanc & Duplessy 1982; Kastens 1992; Aharon et al. 1993). Glacially induced changes in the SCIW velocity are again proposed to account for the winnowing episodes in the latest Miocene sediment from Hole 593.

After 5 Ma, the dramatic increase in sand content and slightly reduced sedimentation rates are inferred to be due to a continued increase in winnowing intensity over the Challenger Plateau. The 30% reduction in sand content through the early late Pliocene is inferred to be the result of a lag in circulation changes from the early Pliocene warm period (where circulation would be assumed to be less intense) into renewed winnowing as the global climate system cooled further after this warm interval (Fig. 12). As with the Miocene climate optimum (Fig. 12), the textural changes appear to lag the climate/circulation changes, likely the result of inertia in the system as the climate changes state. Winnowing then increases through the last 3 m.y. of the Hole 593 record as a result of increased SCIW flow velocities associated with increasing global ice volume and Quaternary glaciations.

CONCLUSIONS

Sediments from Hole 593, presently bathed by Antarctic Intermediate Water on the outer edge of Challenger Plateau (1068 m), comprise a continuous section of Neogene pelagic carbonate nannofossil oozes. The mud-sized fraction (<63 μm) comprises 75–90% of the Miocene sediment, decreasing to 50–75% in the Pliocene and Quaternary sediments. The mud fraction consists mainly of nannofossil placoliths, with c. 5–10% juvenile foraminifera, and minor amounts of clay minerals. Adult foraminifera dominate the sand fraction, together with small quantities of bolboforms and siliciclastic material.

Current winnowing of early–late Miocene sediments on Challenger Plateau is evident in the sediment texture data from a number of features: (1) changes in the mud (<63 μm) content at several intervals: 19–17.5 Ma, 16.5–14.5 Ma, 9.5–8 Ma, and after 5 Ma; (2) the presence of a condensed sedimentary section from 18 to 14 Ma, enriched in foraminifera; (3) the selective removal of fine silt to very coarse clay sizes (13–3 μm), but not smaller grains; and (4) an up-core reduction in the mean grain size of the mud fraction. Unlike deep-sea sediments with much larger quantities of terrigenous material, in the pelagic carbonate oozes at Site 593 the grains <10 μm in size do not appear to have acted cohesively, presumed to reflect the composition of the silt-sized calcitic nannofossil placoliths. Winnowing of pelagic carbonate ooze is more likely a reflection of the hydrodynamic properties of nannofossil placoliths and the ease with which they are mobilised by fluctuating water velocity.

A trimodal grain-size distribution within the mud fraction is consistent throughout the Neogene record, and reflects the composition of the sediment: (1) coarse silt mode (53–37 μm)—juvenile foraminifera; (2) very fine silt mode (6.6–4.7 μm)—nannofossil placoliths; and (3) fine clay mode (0.35–0.4 μm)—placolith lathes (and clay minerals). Winnowing episodes have mainly selectively removed grains contributing to the very fine silt mode. The shift in the grain size of the very fine silt mode from 6.6 to 4.7 μm over the interval c. 7.5–6 Ma, is interpreted as the late Miocene "small *Reticulofenestra* interval", where nannofossil placoliths record a size reduction. This interval has not been previously reported from the region, and the textural size change provides an independent measure of the placolith size reduction.

Increases in the winnowing potential of SCIW, the Neogene equivalent to AAIW, are linked to more invigorated circulation over time, especially during the glacial Miocene (Mi) zones. These are associated with Antarctic cooling and ice-sheet development, specifically the East Antarctic Ice Sheet, during the winnowing from c. 19 to 12.6 Ma (Mi1b–Mi4), and the West Antarctic Ice Sheet during the winnowing from c. 11 to 9.3 Ma (Mi5–Mi7), and subsequently the appearance of Northern Hemisphere ice sheets from 5 Ma onwards. The increasing textural fluctuations during the last 5 m.y. are in part due to the addition of megascopic tephras from the New Zealand continent to the sediments on the Challenger Plateau, and also to the more extreme climate fluctuations over this interval, evident in many global paleoceanographic reconstructions.

ACKNOWLEDGMENTS

We thank the several students who helped run the 2500 Lasersizer analyses underpinning this study, and Lionel Carter (NIWA) and Bob Carter (James Cook University) for helpful review comments of an early draft manuscript. Reviewers Kerry Swanson (University of Canterbury) and Peter Davies (University of Sydney) made constructive comments that improved the paper. Financial support for this work came from Marsden Fund contract UOW523 to the University of Waikato (PhD funding for PJC and MPC), and Foundation for Research, Science and Technology funding to Institute of Geological and Nuclear Sciences (contract C05X0005).

NOTE ADDED IN PROOF: Recent revision of the Site 593 biostratigraphy (Field, Crundwell, et al. in prep. "The signature of middle Miocene climate change in the New Zealand (Southwest Pacific) region) has now amended the condensed section description to include a 2 m.y. hiatus at the top of the "orange unit". This does not substantially alter the final conclusions of this paper and has beneficial implications for the winnowing intensity changes proposed herein. The consequence of this revision will be documented in future interpretations of the Site 593 datasets.

REFERENCES

Aharon, P.; Goldstein, S. L.; Wheeler, C. W.; Jacobson, G. 1993: Sea-level events in the South Pacific linked with the Messinian salinity crisis. *Geology 21*: 771–775.

Backman, J.; Raffi, I. 1997: Calibration of Miocene nannofossil events to orbitally tuned cyclostratigraphies from Ceara Rise. *In*: Shackleton, N. J.; Curry, W. B.; Richter, C.; Bralower, T. J. *ed. Proceedings of the Ocean Drilling Program, Scientific Results 154*. College Station, TX., Ocean Drilling Program. Pp. 83–99.

Bennett, A. F. 1983: The south Pacific including the East Australian Current. *In*: Robinson, A. R. *ed*. Eddies in marine science. Springer-Verlag. Pp. 219–244.

Berger, W. H. 1970: Planktonic foraminifera: selective solution and the lysocline. *Marine Geology 8*: 111–138.

Berger, W. H.; Winterer, E. L. 1974: The concepts 'Carbonate Line' and 'Compensation Surface'. *In*: Hsü, K. J.; Jenkyns, H. C. *ed*. Pelagic sediments: on land and under the sea. Vol 1. Special Publication of the International Association of Sedimentologists. Blackwell. Pp. 11–48.

Berggren, W. A.; Hilgen, F. J.; Langereis, C. G.; Kent, D. V.; Obradovich, J. D.; Raffi, I.; Raymo, M. E.; Shackleton, N. J. 1995a: Late Neogene chronology: new perspectives in high-resolution stratigraphy. *Geological Society of America Bulletin 107*: 1272–1287.

Berggren, W. A.; Kent, D. V.; Swisher, C. C. III; Aubry, M-P. 1995b: A revised Cenozoic geochronology and chronostratigraphy. *In*: Berggren, W. A.; Kent, D. V.; Aubry, M-P.; Hardenbol, J. *ed*. Geochronology, time scales and global stratigraphic correlation. *SEPM Special Publication 54*. Society for Sedimentary Geology. Pp. 129–212.

Blanc, P-L.; Duplessy, J-C. 1982: The deep-water circulation during the Neogene and the impact of the Messinian salinity crisis. *Deep-Sea Research 29*: 1391–1414.

Boersma, A. 1986: Biostratigraphy and biogeography of Tertiary bathyal benthic foraminifers: Tasman Sea, Coral Sea, and on the Chatham Rise (Deep Sea Drilling Project, Leg 90). *In*: Kennett, J. P.; von der Borch, C. C. and others *ed*. *Initial reports of the Deep Sea Drilling Project 90*. Washington, U.S. Government Printing Office. Pp. 961–1035.

Bohrmann, G.; Ehrmann, W. U. 1991: Analysis of sedimentary facies using bulk mineralogical characteristics of Cretaceous to Quaternary sediments from the Kerguelen Plateau: Sites 737, 738, and 744. *In*: Barron, J.; Larsen, B. and others *ed. Proceedings of the Ocean Drilling Program, Scientific Results 119*. College Station, TX, Ocean Drilling Program. Pp. 211–237.

Bradford, J. M.; Roberts, P. E. 1978: Distribution of reactive phosphorus and plankton in relation to upwelling and surface circulation around New Zealand. *New Zealand Journal of Marine and Freshwater Research 12*: 1–15.

Burns, R. E.; Andrews, J. E. 1973: Regional aspects of Deep Sea Drilling in the southwest Pacific. *In*: Burns, R. E.; Andrews, J. E. and others *ed*. *Initial reports of the Deep Sea Drilling Project 21*. Washington, U.S. Government Printing Office. Pp. 897–906.

Carter, L.; Garlick, R. D.; Sutton, P.; Chiswell, S. M.; Oien, N. A.; Stanton, B. R. 1998a: Ocean circulation New Zealand. *NIWA Chart Miscellaneous Series 76*. Wellington, National Institute of Water and Atmospheric Research.

Carter, R. M.; McCave, I. N.; Richter, C. 1998b: Ocean Drilling Program Leg 181 preliminary report Southwest Pacific Gateways. *Preliminary Report No. 81*. Ocean Drilling Program.

Caulet, J-P. 1986: Radiolarians from the southwest Pacific. *In*: Kennett, J. P.; von der Borch, C. C. and others *ed*. *Initial reports of the Deep Sea Drilling Project 90*. Washington, U.S. Government Printing Office. Pp. 835–861.

Ciesielski, P. F.; Ledbetter, M. T.; Ellwood, B. B. 1982: The development of Antarctic glaciation and the Neogene paleoenvironment of the Maurice Ewing Bank. *Marine Geology 46*: 1–51.

Circum-Pacific Map Project 1978: Geographic map of the Circum-Pacific region: southwest quadrant. Tulsa, Oklahoma, American Association of Petroleum Geologists.

Collins, L. S.; Coates, A. G.; Berggren, W. A.; Aubry, M-P.; Zhang, J. 1996: The late Miocene Panama isthmian strait. *Geology 24*: 687–690.

Cooke, P. J. 2002: Aspects of Neogene palaeoceanography in the southern Tasman Sea (DSDP Site 593). Unpublished PhD thesis, lodged in the Library, University of Waikato, Hamilton, New Zealand. 334 p.

Cooke, P. J.; Nelson, C. S.; Crundwell, M. P.; Spiegler, D. 2002: *Bolboforma* as monitors of Cenozoic palaeoceanographic changes in the Southern Ocean. *Palaeogeography, Palaeoclimatology, Palaeoecology 188*: 73–100.

Crundwell, M. P. 2004: New Zealand late Miocene: biostratigraphy and biochronology studies of planktic foraminifers and bolboforms at oceanic Sites 593 and 1123, and selected onland sections. Unpublished PhD thesis, University of Waikato, Hamilton, New Zealand.

Drewry, D. J. *ed*. 1983: Antarctica, glaciological and geophysical folio (map). Cambridge, University of Cambridge, Scott Polar Research Institute.

Dudley, W. C.; Nelson, C. S. 1989: Quaternary surface-water stable isotope signal from calcareous nannofossils at DSDP Site 593, Southern Tasman Sea. *Marine Micropaleontology 13*: 353–373.

Elkington, E. S.; Cooke, P. J.; Nelson, C. S.; Stone, H. S.; Field, B.; Crundwell, M. P.; Rogers, K. 2000: Early to middle Miocene palaeoceanography of the Tasman Sea from stable isotopic and textural records. *Geological Society of New Zealand Miscellaneous Publication 108A*. Wellington, Geological Society of New Zealand. P. 41.

Ellwood, B. B.; Ledbetter, M. T. 1977: Antarctic Bottom Water fluctuations in the Vema Channel: effects of velocity changes on particle alignment and size. *Earth and Planetary Science Letters 35*: 189–198.

Ellwood, B. B.; Ledbetter, M. T.; Johnson, D. A. 1979: Sedimentary fabric: a tool to delineate a high-velocity zone within a deep western Indian Ocean bottom current. *Marine Geology 33*: M51–M55.

Elmstrom, K. M.; Kennett, J. P. 1986: Late Neogene paleoceanographic evolution of Site 590: Southwest Pacific. *In*: Kennett, J. P.; von der Borch, C. C. and others *ed*. *Initial reports of the Deep Sea Drilling Project 90*. Washington, U.S. Government Printing Office. Pp. 1361–1381.

Flores, J-A.; Sierro, F-J. 1989: Calcareous nannoflora and planktonic foraminifera in the Tortonian-Messinian boundary interval of East Atlantic DSDP sites and their relation to Spanish and Moroccan sections. *In*: Crux, J. A.; van Heck, S. E. *ed*. Nannofossils and their applications. Proceedings of the International Nannofossil Association Conference, London 1987. Ellis Horwood Limited. Pp. 249–266.

Flores, J-A.; Sierro, F-J.; Glaçon, G. 1992: Calcareous plankton analysis in the pre-evaporitic sediments of the ODP Site 654 (Turrhenian Sea, Western Mediterranean). *Micropaleontology 38*: 279–288.

Flower, B. P.; Kennett, J. P. 1994: The middle Miocene climatic transition: East Antarctic ice sheet development, deep ocean circulation and global carbon cycling. *Palaeogeography, Palaeoclimatology, Palaeoecology 108*: 537–555.

Flower, B. P.; Kennett, J. P. 1995: Middle Miocene deepwater paleoceanography in the southwest Pacific: relations with East Antarctic Ice Sheet development. *Paleoceanography 10*: 1095–1112.

Folk, R. L. 1968: Petrology of sedimentary rocks. Austin, Texas, Hemphill's. 170 p.

Folk, R. L.; Ward, W. C. 1957: Brazos River bar: a study in the significance of grain size parameters. *Journal of Sedimentary Petrology 27*: 3–26.

Gardner, J. V.; Dean, W. E.; Bisagno, L.; Hemphill, E. 1986a: Late Neogene and Quaternary coarse-fraction and carbonate stratigraphies for Site 586 on Ontong-Java Plateau and Site 591 on Lord Howe Rise. *In*: Kennett, J. P.; von der Borch, C. C. and others *ed*. *Initial reports of the Deep Sea Drilling Project 90*. Washington, U.S. Government Printing Office. Pp. 1201–1224.

Gardner, J. V.; Nelson, C. S.; Baker, P. A. 1986b: Distribution and character of Pale Green Laminae in sediments from Lord Howe Rise: a probable late Neogene and Quaternary tephrostratigraphic record. *In*: Kennett, J. P.; von der Borch, C. C. and others *ed*. *Initial reports of the Deep Sea Drilling Project 90*. Washington, U.S. Government Printing Office. Pp. 1145–1161.

Garner, D. M. 1962: Analysis of hydrological observations in the New Zealand region, 1874–1955. *DSIR Bulletin 144 (NZOI Memoir No. 9)*. Wellington, New Zealand, Department of Scientific and Industrial Research. 45 p.

Garner, D. M. 1967: Hydrology of the south-east Tasman Sea. *DSIR Bulletin 181 (NZOI Memoir No. 48)*. Wellington, New Zealand, Department of Scientific and Industrial Research. 40 p.

Garner, D. M.; Ridgway, N. M. 1965: Hydrology of New Zealand offshore waters. *DSIR Bulletin 162 (NZOI Memoir No. 12)*. Wellington, New Zealand, Department of Scientific and Industrial Research. 63 p.

Garrison, R. E. 1981: Diagenesis of oceanic carbonate sediments: a review of the DSDP prespective. *SEPM Special Publication 32*: 181–207.

Gasol, J. M.; del Giorgio, P. A.; Duarte, C. M. 1997: Biomass distribution in marine planktonic communities. *Limnology and Oceanography 42*: 1353–1363.

Gorsline, D. S. 1984: A review of fine-grained sediment origins, characteristics, transport and deposition. *In*: Stow, D. A. V.; Piper, D. J. W. *ed*. Fine-grained sediments: deep-water processes and facies. *Geological Society Special Publication 15*. Oxford, Blackwell Scientific. Pp. 17–34.

Hamilton, L. J. 1990: Temperature inversions at intermediate depths in the Antarctic Intermediate Waters of the south-western Pacific. *Australian Journal of Marine and Freshwater Research 41*: 325–351.

Haq, B. U. and others 1980: Late Miocene marine carbon-isotopic shift and synchroneity of some phytoplanktonic biostratigraphic events. *Geology 8*: 427–431.

Head, P. S.; Nelson, C. S. 1994: A high-resolution oxygen isotope record for the past 6.4 million years at DSDP Site 593, Challenger Plateau, southern Tasman Sea. *In*: van der Lingen, G. J.; Swanson, K. M.; Muir, R. J. *ed*. Evolution of the Tasman Sea Basin. Rotterdam, A. A. Balkema. Pp. 159–179.

Heath, R. A. 1985: A review of the physical oceanography of the seas around New Zealand—1982. *New Zealand Journal of Marine and Freshwater Research 19*: 79–124.

Hesse, P. P. 1994: The record of continental dust from Australia in Tasman Sea sediments. *Quaternary Science Reviews 13*: 257–272.

Hodell, D. A.; Elmstrom, K. M.; Kennett, J. P. 1986: Latest Miocene benthic $\delta^{18}O$ changes, global ice volume, sea level and the 'Messinian salinity crisis'. *Nature 320*: 411–414.

House, M. A.; Rea, D. K.; Janecek, T. R. 1991: Grain-size record of ocean current winnowing in Oligocene to Pleistocene ooze, Broken Ridge, southeastern Indian Ocean. *In*: Weissel, J.; Peirce, J.; Taylor, E.; Alt, J. and others *ed*. *Proceedings of the Ocean Drilling Program, Scientific Results 121*. College Station, TX, Ocean Drilling Program. Pp. 211–218.

Howe, J. A.; Pudsey, C. J. 1999: Antarctic Circumpolar Deep Water: a Quaternary paleoflow record from the northern Scotia Sea, South Atlantic Ocean. *Journal of Sedimentary Research 69*: 847–861.

Huang, T. C.; Watkins, N. D. 1977: Contrasts between the Brunhes and Matuyama sedimentary records of bottom water activity in the South Pacific. *Marine Geology 23*: 113–132.

Jenkins, C. J. 1985: Erosion and deposition at abyssal depths in the Tasman Sea: a seismic stratigraphic study of bottom-current patterns. *Ocean Science Institute Report 4*. Sydney, University of Sydney. 53 p.

Jenkins, C. J. 1992: Abyssal sediment drifts, erosion and history of bottom water flow in the Tasman Sea southwest of New Zealand. *Australian Journal of Earth Sciences 39*: 195–210.

Kastens, K. A. 1992: Did glacio-eustatic sea level drop trigger the Messinian salinity crisis? New evidence from ocean drilling program site 654 in the Tyrrhenian Sea. *Paleoceanography 7*: 333–356.

Keigwin, L. D. Jr; Shackleton, N. J. 1980: Uppermost Miocene carbon isotope stratigraphy of a piston core in the equatorial Pacific. *Nature 284*: 613–614.

Kennett, J. P.; von der Borch, C. C. 1986a: Southwest Pacific Cenozoic paleoceanography. *In*: Kennett, J. P.; von der Borch, C. C. and others *ed*. *Initial reports of the Deep Sea Drilling Program 90*. Washington, U.S. Government Printing Office. Pp. 1493–1517.

Kennett, J. P.; von der Borch, C. C. 1986b: *Initial reports of the Deep Sea Drilling Project 90*. Washington, U.S. Government Printing Office.

Kennett, J. P.; Keller, G.; Srinivasan, M. S. 1985: Miocene planktonic foraminiferal biogeography and paleoceanographic development of the Indo-Pacific region. *In*: Kennett, J. P. *ed*. The Miocene ocean: paleoceanography and biogeography. *Geological Society of America Memoir 163*: 197–236.

Leg 90 Shipboard Scientific Party 1986: Site 593: Challenger Plateau. *In*: Kennett, J. P.; von der Borch, C. C. and others *ed*. *Initial reports of the Deep Sea Drilling Project 90*. Washington, U.S. Government Printing Office. Pp. 551–651.

Leinen, M. 1979: Biogenic silica accumulation in the central equatorial Pacific and its implications for Cenozoic paleoceanography: summary. *Geological Society of America Bulletin, Part 1*, *90*: 801–803.

Lohman, W. H. 1986: Calcareous nannoplankton biostratigraphy of the southern Coral Sea, Tasman Sea, and southwestern Pacific Ocean, Deep Sea Drilling Project Leg 90: Neogene and Quaternary. *In*: Kennett, J. P.; von der Borch, C. C. and others *ed*. *Initial reports of the Deep Sea Drilling Project 90*. Washington, U.S. Government Printing Office. Pp. 763–793.

Lyle, M.; Dadey, K. A.; Farrell, J. W. 1995: The late Miocene (11–8 Ma) eastern Pacific carbonate crash: evidence for reorganization of deep-water circulation by the closure of the Panama Gateway. *In*: Pisias, N. G.; Mayer, L. A.; Janecek, T. R.; Palmer-Julson, A.; van Andel, T. H. *ed*. *Proceedings of the Ocean Drilling Program, Scientific Results 138*. College Station, TX, Ocean Drilling Program. Pp. 821–838.

McCave, I. N. 1984: Erosion, transport and deposition of fine-grained marine sediments. *In*: Stow, D. A. V.; Piper, D. J. W. *ed*. Fine-grained sediments: deep-water processes and facies. *Geological Society Special Publication 15*. Oxford, Blackwell Scientific. Pp. 35–69.

McCave, I. N.; Manighetti, B.; Robinson, S. G. 1995: Sortable silt and fine sediment size/composition slicing: parameters for palaeocurrent speed and palaeoceanography. *Paleoceanography 10*: 593–610.

Manighetti, B.; McCave, I. N. 1995: Late glacial and Holocene palaeocurrents around Rockall Bank, NE Atlantic Ocean. *Paleoceanography 10*: 611–626.

Marshall, P.; Kidson, E. 1929: The dust-storm of October, 1928. *New Zealand Journal of Science and Technology 10*: 291–299.

Martínez, J. I. 1994: Late Pleistocene carbonate dissolution patterns in the Tasman Sea. *In*: van der Lingen, G. J.; Swanson, K. M.; Muir, R. J. *ed*. Evolution of the Tasman Sea Basin. Rotterdam, A. A. Balkema. Pp. 215–228.

Miller, K. G.; Wright, J. D.; Fairbanks, R. G. 1991: Unlocking the Ice House: Oligocene-Miocene oxygen isotopes, eustacy, and margin erosion. *Journal of Geophysical Research 96(B4)*: 6829–6848.

Morgans, H. E. G.; Scott, G. H.; Beu, A. G.; Graham, I. J.; Mumme, T. C.; St George, W.; Strong, C. P. 1996: New Zealand Cenozoic time scale. *Science Report 96/38*. Institute of Geological & Nuclear Sciences.

Murphy, R. J.; Pinkerton, M. H.; Richardson, K. M.; Bradford-Grieve, J. M.; Boyd, P. W. 2001: Phytoplankton distributions around New Zealand derived from SeaWiFS remotely-sensed ocean colour data. *New Zealand Journal of Marine and Freshwater Research 35*: 353–362.

Mycke, B.; Emeis, K-C.; Degens, E. T. 1986: Diagenesis of organic compounds in Hole 593, Leg 90 (Tasman Sea). *In*: Kennett, J. P.; von der Borch, C. C. and others *ed*. *Initial reports of the Deep Sea Drilling Project 90*. Washington, U.S. Government Printing Office. Pp. 1265–1269.

Naish, T. R. 1996: High-resolution sequence stratigraphy, sedimentology, paleoecology, and chronology of the Pliocene-Pleistocene (c. 2.6–1.7 Ma) Rangitikei Group, Wanganui Basin, New Zealand. Unpublished DPhil thesis, lodged in the Library, University of Waikato, Hamilton, New Zealand. 300 p.

Nelson, C. S. 1986a: Lithostratigraphy of Deep Sea Drilling Project Leg 90 drill sites in the southwest Pacific: an overview. *In*: Kennett, J. P.; von der Borch, C. C. and others *ed*. *Initial reports of the Deep Sea Drilling Project 90*. Washington, U.S. Government Printing Office. Pp. 1471–1491.

Nelson, C. S. 1986b: Bioturbation in middle bathyal, Cenozoic nannofossil oozes and chalks, Southwest Pacific. *In*: Kennett, J. P.; von der Borch, C. C. and others *ed*. *Initial reports of the Deep Sea Drilling Project 90*. Washington, U.S. Government Printing Office. Pp. 1189–1200.

Nelson, C. S.; Cooke, P. J. 2001: History of oceanic front development in the New Zealand sector of the Southern Ocean during the Cenozoic—a synthesis. *New Zealand Journal of Geology and Geophysics 44*: 535–553.

Nelson, C. S.; Froggatt, P. C.; Gosson, G. J. 1986a: Nature, chemistry, and origin of late Cenozoic megascopic tephras in Leg 90 cores from the southwest Pacific. *In*: Kennett, J. P.; von der Borch, C. C. and others *ed*. *Initial reports of the Deep Sea Drilling Project 90*. Washington, U.S. Government Printing Office. Pp. 1161–1173.

Nelson, C. S.; Hendy, C. H.; Dudley, W. C. 1986b: Quaternary isotope stratigraphy of Hole 593, Challenger Plateau, south Tasman Sea: preliminary observations based on foraminifers and calcareous nannofossils. *In*: Kennett, J. P.; von der Borch, C. C. and others *ed*. *Initial reports of the Deep Sea Drilling Project 90*. Washington, U.S. Government Printing Office. Pp. 1413–1424.

Nelson, C. S.; Hendy, C. H.; Cuthbertson, A. M. 1994: Oxygen isotope evidence for climatic contrasts between Tasman Sea and Southwest Pacific Ocean during the late Quaternary. *In*: van der Lingen, G. J.; Swanson, K. M.; Muir, R. J. *ed*. Evolution of the Tasman Sea Basin. Rotterdam, A. A. Balkema. Pp. 181–196.

Oser, R. K. 1972: Sedimentary components of Northwest Pacific pelagic sediments. *Journal of Sedimentary Petrology 42*: 461–467.

Park, Y-H.; Gamberoni, L.; Charriaud, E. 1993: Frontal structure, water masses, and circulation in the Crozet Basin. *Journal of Geophysical Research 98(C7)*: 12361–12385.

Perry, A. H.; Walker, J. M. 1977: The ocean-atmosphere system. London, Longman Group Ltd. 160 p.

Raffi, I.; Flores, J-A. 1995: Pleistocene through Miocene calcareous nannofossils from Eastern Equatorial Pacific Ocean (Leg 138). *In*: Pisias, N. G.; Mayer, L. A.; Janecek, T. R.; Palmer-Julson, A.; van Andel, T. H. *ed*. *Proceedings of the Ocean Drilling Program, Scientific Results 138*. College Station, TX, Ocean Drilling Program. Pp. 233–286.

Rawle, A. 1995: The basic principles of particle size analysis. Technical Paper, Malvern Instruments Ltd. 8 p.

Reid, J. L. 1986: On the total geostrophic circulation of the South Pacific Ocean: flow patterns, tracers and transport. *Progress in Oceanography 16*: 1–61.

Rio, D.; Fornaciari, E.; Raffi, I. 1990: Late Oligocene through early Pleistocene calcareous nannofossils from western equatorial Indian Ocean (Leg 115). *In*: Duncan, R. A.; Backman, J.; Peterson, L. C. and others *ed*. *Proceedings of the Ocean Drilling Program, Scientific Results 115*. College Station, TX, Ocean Drilling Program. Pp. 175–235.

Robert, C.; Stein, R.; Acquaviva, M. 1986: Cenozoic evolution and significance of clay associations in the New Zealand region of the south Pacific, Deep Sea Drilling Project, Leg 90. *In*: Kennett, J. P.; von der Borch, C. C. and others *ed*. *Initial reports of the Deep Sea Drilling Project 90*. Washington, U.S. Government Printing Office. Pp. 1225–1238.

Robinson, S. G.; McCave, I. N. 1994: Orbital forcing of bottom-current enhanced sedimentation on Feni Drift, NE Atlantic, during the mid-Pleistocene. *Paleoceanography 9*: 943–972.

Rochford, D. J. 1983: Origins of water within warm-core eddies of the western Tasman Sea. *Australian Journal of Marine and Freshwater Research 34*: 525–534.

Rodman, M. R.; Gordon, A. L. 1982: Southern Ocean bottom water of the Australian-New Zealand Sector. *Journal of Geophysical Research 87(C8)*: 5771–5778.

Schlich, R.; Wise, S. W. Jr 1992: The geologic and tectonic evolution of the Kerguelen Plateau: an introduction to the scientific results of Leg 120. *In*: Wise, S. W. Jr; Schlich, R. and others *ed*. *Proceedings of the Ocean Drilling Program, Scientific Results 120 (Part 1)*. College Station, TX, Ocean Drilling Program. Pp. 5–30.

Shackleton, N. J.; Kennett, J. P. 1975: Paleotemperature history of the Cenozoic and the initiation of Antarctic glaciation: oxygen and carbon isotope analysis in DSDP Sites 277, 279, and 281. *In*: Kennett, J. P.; Houtz, R. E. and others *ed*. *Initial reports of the Deep Sea Drilling Project 29*. Washington, U.S. Government Printing Office. Pp. 743–755.

Shackleton, N. J.; Crowhurst, S.; Hagelberg, T.; Pisias, N. G.; Schneider, D. A. 1995: A new late Neogene time scale: application to Leg 138 sites. *In*: Pisias, N. G.; Mayer, L. A.; Janecek, T. R.; Palmer-Julson, A.; van Andel, T. H. *ed*. *Proceedings of the Ocean Drilling Program, Scientific Results 138*. College Station, TX, Ocean Drilling Program. Pp. 73–101.

Southard, J. B.; Young, R. A.; Hollister, C. D. 1971: Experimental erosion of calcareous ooze. *Journal of Geophysical Research 76(24)*: 5903–5909.

Stanton, B. R. 1973: Circulation along the eastern boundary of the Tasman Sea. *In*: Fraser, R. *ed*. Oceanography of the South Pacific 1972. Wellington, New Zealand National Commission for UNESCO. Pp. 141–147.

Stanton, B. R. 1979: The Tasman Front. *New Zealand Journal of Marine and Freshwater Research 13*: 201–214.

Stein, R.; Robert, C. 1986: Siliclastic sediments at Sites 588, 590, and 591: Neogene and Paleogene evolution in the southwest Pacific and Australian climate. *In*: Kennett, J. P.; von der Borch, C. C. and others *ed*. *Initial reports of the Deep Sea Drilling Project 90*. Washington, U.S. Government Printing Office. Pp. 1437–1455.

Stramma, L.; Peterson, R. G.; Tomczak, M. 1995: The South Pacific Current. *Journal of Physical Oceanography 25*: 77–91.

Sutherland, F. L. 1994: Tasman Sea evolution and hotspot trail. *In*: van der Lingen, G. J.; Swanson, K. M.; Muir, R. J. *ed*. Evolution of the Tasman Sea Basin. Rotterdam, A. A. Balkema. Pp. 35–52.

Swanson, K.; van der Lingen, G. 1997: Late Quaternary ostracod and planktonic foraminiferal dissolution signals from the eastern Tasman Sea—palaeoenvironmental implications. *Palaeogeography, Palaeoclimatology, Palaeoecology 131*: 303–314.

Takayama, T. 1993: Notes on Neogene calcareous nannofossil biostratigraphy of the Ontong Java Plateau and size variations of *Reticulofenestra* coccoliths. *In*: Berger, W. H.; Kroenke, L. W.; Mayer, L. A. and others *ed*. *Proceedings of the Ocean Drilling Program, Scientific Results 130*. College Station, TX, Ocean Drilling Program. Pp. 179–229.

Thiede, J. 1979: Wind regimes over the late Quaternary southwest Pacific Ocean. *Geology 7*: 259–262.

Tomczak, M.; Godfrey, J. S. 1994: Regional oceanography: an introduction. Oxford, Pergamon. 422 p.

van Andel, T. H. 1973: Texture and dispersal of sediments in the Panama Basin. *Journal of Geology 81*: 434–457.

Varney, M. 1996: The marine carbonate system. *In*: Summerhayes, C. P.; Thorpe, S. A. *ed*. Oceanography an illustrated guide. London, Manson Publishing. Pp. 183–194.

Vincent, E.; Killingley, J. S.; Berger, W. H. 1980: The magnetic Epoch-6 carbon shift: a change in the ocean's $^{13}C/^{12}C$ ratio 6.2 million years ago. *Marine Micropaleontology 5*: 185–203.

Vincent, W. F.; Howard-Williams, C. 1991: Distribution and biological properties of oceanic water masses around the South Island, New Zealand. *New Zealand Journal of Marine and Freshwater Research 25*: 21–42.

Windom, H. L. 1969: Atmospheric dust records in permanent snowfields: implications to marine sedimentation. *Geological Society of America Bulletin 80*: 761–782.

Wood, R. A. 1993: The Challenger Plateau. *In*: Ballance, P. F. *ed*. South Pacific sedimentary basins. Sedimentary basins of the world, 2. Amsterdam, Elsevier Science Publishers, B.V. Pp. 351–364.

Woodruff, F.; Savin, S. M. 1991: Mid-Miocene isotope stratigraphy in the deep sea: high-resolution correlations, paleoclimatic cycles and sediment preservation. *Paleoceanography 6*: 755–806.

Wright, J. D.; Miller, K. G. 1992: Miocene stable isotope stratigraphy, Site 747, Kerguelen Plateau. *In*: Wise, S. W. Jr; Schlich, R. and others *ed*. *Proceedings of the Ocean Drilling Program, Scientific Results 120*. College Station, TX, Ocean Drilling Program. Pp. 855–865.

Wyrtki, K. 1961: The flow of water into the deep sea basins of the western south Pacific Ocean. *Australian Journal of Marine and Freshwater Research 12*: 1–16.

Wyrtki, K. 1962: The subsurface water masses in the western south Pacific Ocean. *Australian Journal of Marine and Freshwater Research 13*: 18–47.

Yoder, J. A.; Ackleson, S. G.; Barber, R. T.; Flament, P.; Balch, W. M. 1994: A line in the sea. *Nature 371*: 689–692.

Young, J. R. 1990: Size variation of Neogene *Reticulofenestra* coccoliths from Indian Ocean DSDP cores. *Journal of Micropalaeontology 9*: 71–86.